TECHNICAL UNIVERSITY OF CRETE

SCHOOL OF ELECTRICAL AND COMPUTER ENGINEERING

Study of Dielectric Strength of Medium Voltage Cables

Diploma Thesis

Athina-Konstantina Antoniou

Thesis Committee:

Georgios Peppas, Assistant Professor – Thesis Supervisor

Konstantinos Gyftakis, Associate Professor

Eftychios Koutroulis, Professor

July 2025

ABSTRACT

Cables in medium voltage networks are exposed to two distinct electrical challenges: the continuous stress of normal operation and the abrupt, high-energy surges produced by lightning or switching events. Although the core insulation provides the primary dielectric barrier, the outer jacket frequently proves to be the first point of weakness during such fast transients. This study investigates the jacket's response to 1,2/50 μs lightning impulses and demonstrates how material formulation, surface condition, and construction details govern breakdown behavior.

Impulse testing was conducted on five types of cable with different nominal voltages, varying jacket compounds (PVC, HDPE, MDPE, PPS+HDPE) and geometry, using a single stage impulse voltage generator. Samples were immersed in insulating oil and subjected to gradually increasing impulses. Oscilloscope traces, paired with visual inspection, confirmed breakdown events. Waveform compliance with IEC 60060-1 was verified via measurements and the generator was also simulated using ATP-EMTP.

Breakdown voltages were evaluated through GEV analysis, yielding U_{10}, U_{50}, and U_{90} levels for each cable. Normalized breakdown field strength (kV/mm) was calculated by dividing breakdown voltage by the measured jacket thickness, offering a geometry-independent performance metric. Additionally, breakdown timing was analyzed to understand how and when insulation failure occurs within the impulse window, giving an indication of the tests and samples consistency.

The findings offer clearly defined dielectric performance benchmarks for commonly used MV cable jackets and present a reproducible laboratory procedure encompassing sample preparation, waveform validation, and statistical breakdown evaluation. By quantifying impulse withstand limits and clarifying failure patterns under transient conditions, this work contributes to more robust oversheath assessment and supports the development of testing frameworks that better reflect real-world electrical stresses.

Keywords: ATP-EMTP, Cable Jacket, IEC Standards, Impulse Testing, Insulation Breakdown, Marx Generator, Medium Voltage Cables, Oil Immersion, Surface Discharge, GEV Distribution

ACKNOWLEDGEMENTS

First and foremost**,** in this many-year academic journey, a path filled with challenges, growth, and moments of deep introspection, I wish to express my profound gratitude to those who stood by me and shaped this thesis into what it has become.

My deepest thanks go to my supervisor, Georgios Peppas, for their continuous support and guidance throughout this process. His insight, encouragement, and thoughtful feedback have not only influenced the course of this research but have also helped me grow as a thinker and researcher. Most of all, I am profoundly grateful to him for believing in me.

I owe special thanks to Michail Pitsikalis, whose unwavering support, insightful guidance, and hands-on assistance were instrumental throughout this journey. Without his help, this thesis would not have taken the shape it had, his contributions were not only practical but deeply encouraging at every critical stage.

To the family of ELEMKO, I extend my warmest appreciation. Their generosity in granting access to their laboratory facilities and for the hands-on guidance they provided during the experimental phases of this work. Their trust and support were instrumental in bringing many of the practical aspects of this research to life and greatly enriched my learning experience. Especially, I am sincerely thankful to Mr. Nikolaos Kokkinos, Evagelos Senis, and Ioannis Koutsoubis for their valuable contributions. Their technical expertise, insightful suggestions, and willingness to share their time and energy significantly enhanced the depth and quality of this thesis, especially during critical moments.

Special recognition goes to George Messaritakis, who undertook his thesis alongside mine and became a true companion in this process. Our shared experiences, countless hours spent in the lab, long discussions, and ongoing encouragement, fostered a sense of friendship and mutual support that made the journey not only more manageable, but also genuinely rewarding.

To my family, thank you for your endless support and for being my anchor through it all. Your unwavering faith, quiet sacrifices, and constant encouragement were the foundation upon which

this thesis stands. To my friends, I’m grateful for every light-hearted moment, every conversation that helped me pause, and every word of support that lifted my spirits when I needed it most.

TABLE OF CONTENTS

LIST OF ACRONYMS

ASTM	American Society for Testing and Materials
CIGRE	International Council on Large Electric Systems
DIN	Deutsche Industrie Norm
ISO	International Organization for Standardization
IEC	International Electrotechnical Commission
IEEE	Institute of Electrical and Electronics Engineers
HV	High Voltage
MV	Medium Voltage

FIGURES LIST

TABLES LIST

CHAPTER 1: INTRODUCTION

1.1 General Overview

Medium-voltage (MV) power cables serve as essential infrastructure within electrical distribution systems, enabling the controlled transfer of energy between substations and end-use facilities across urban, industrial, and rural environments. While the internal insulation layer is often the primary focus in terms of electrical protection, the outer jacket plays a pivotal yet sometimes overlooked role. Beyond serving as a mechanical shield, the jacket acts as a dielectric barrier, safeguarding the cable against moisture penetration, environmental pollutants, and surface discharges.

Despite this multifunctional role, the jacket's electrical behavior, particularly its withstand to high-voltage impulses, has not always been rigorously tested or quantified. Standard design and testing procedures tend to presume that the outer sheath will naturally withstand expected overvoltages, yet real-world field data suggest that impulse-related stress from nearby lightning strikes, can challenge this assumption. As medium voltage cables are increasingly deployed in more exposed or critical environments, there is a growing need to evaluate how well the jacket withstands such non-continuous, high-stress events.

1.2 State of the Art

Contemporary cable testing practices primarily emphasize the electrical and thermal performance of the core insulation, given its direct role in sustaining steady-state operating voltages. The outer jacket, though essential for mechanical protection and environmental sealing, is rarely subjected to rigorous dielectric evaluation. Most standards and manufacturer procedures focus on properties like tensile strength, abrasion resistance, elongation, and size accuracy, while giving little attention to how the jacket performs under fast electrical transients.

This gap in testing methodology leaves potential failure mechanisms undetected, such as embedded conductive particles, surface inhomogeneities, or compromised polymer interfaces,

which may become critical under impulse conditions. Without targeted assessment, such weaknesses may go unnoticed until a failure occurs in service. The absence of jacket-level impulse withstand requirements in widely adopted standards further exacerbates this risk, highlighting the need for a more comprehensive and forward-looking approach to MV cable qualification.

1.3 Thesis Objective

This thesis aims to systematically investigate the dielectric behavior of medium voltage cable jackets when exposed to high voltage impulse conditions. Unlike conventional testing practices that focus primarily on the core insulation, this study centers specifically on the cable jacket and its capacity to resist breakdown during fast-transient electrical events.

The main objectives are to:

- Experimentally determine the breakdown voltage of the outer jacket in multiple MV cable types using standard 1,2/50 μs impulse waveforms.
- Compare performance across different jacket materials and constructions to assess how geometry, thickness, and compound formulation influence dielectric strength.

The findings seek to address a critical gap in current testing methodologies by providing experimentally grounded insights into the performance of MV cable jackets under realistic impulse stress conditions.

1.4 Contribution

This thesis provides new insights into the impulse voltage performance of medium-voltage cable jackets. The key contributions are:

- A comprehensive set of experimental data characterizing impulse breakdown behavior across multiple MV cable types, gathered under repeatable, controlled test conditions.
- Introduction of a thickness-normalized field strength metric (kV/mm) to enable fair comparisons across cables with differing jacket geometries and dimensions.

- Application of GEV statistical analysis to derive U_{10}, U_{50}, and U_{90} breakdown percentiles, thereby quantifying both typical and extreme dielectric performance.
- Time-domain waveform analysis to correlate breakdown initiation with specific regions of the impulse, front or tail, revealing the dynamic vulnerability of certain materials to steep voltage gradients.
- Evidence-based recommendations for enhancing test protocols by incorporating impulse withstand evaluations into jacket qualification procedures, particularly for MV cables deployed in high-risk environments.

These findings contribute to more reliable MV cable designs and support the case for refining existing standards to account for jacket-level dielectric performance.

CHAPTER 2: MEDIUM VOLTAGE CABLES AND TESTING

2.1 Introduction

The extensive use of medium voltage (MV) cable lines in renewable energy systems has brought forth new challenges related to the reliability of underground cable lines. Power transmission lines connecting the renewable energy parks to the rest of the power grid keep getting longer due to the remote and mountainous locations of wind and photovoltaic parks [1]. In such contexts, overhead transmission is often impractical, thereby making underground cabling the preferred approach [2]. However, the substantial lengths along with the location of the renewable energy parks, make the cable lines susceptible to direct lightning strikes and induced lightning surges. This makes the reliability of the cables during lightning transients critical for system performance and operational safety.

This chapter provides a comprehensive overview of MV cable technology and the standardized testing practices used to assess their electrical integrity. It begins with describing the internal structure and materials used in typical MV cable designs, followed by a discussion on the concept of dielectric strength and breakdown mechanisms. The chapter concludes with a detailed review of applicable international standards and testing methodologies, including routine, type, and prequalification tests, with a particular focus on those relevant to dielectric and impulse strength evaluation.

2.2 Overview of Cable Structure and Function

Medium voltage cables are designed to withstand demanding operational conditions by using careful engineered structural elements and materials. Their performance depends not only on the electrical properties of the insulation but also on the mechanical protection, environmental durability, and physical integrity provided by each surrounding layer. A solid understanding of how these components interact is essential for evaluating cable reliability under stress.

2.2.1 Basic Structure of MV Cables

Medium voltage power cables, as specified in technical literature and international standards, follow a concentric, layer-on-layer construction that begins with either a solid or stranded conductor. A thin semiconducting screen is extruded directly over the conductor, after which the main insulation is applied to the thickness required for the rated voltage. The main insulation is immediately covered by a second semiconducting layer, which is bonded to the dielectric. Surrounding this triple-extruded core is a grounded metallic screen. Finally, a tough outer, insulating sheath, the cable jacket seals the assembly. Figure 1 depicts the typical structure of a MV cable [1].

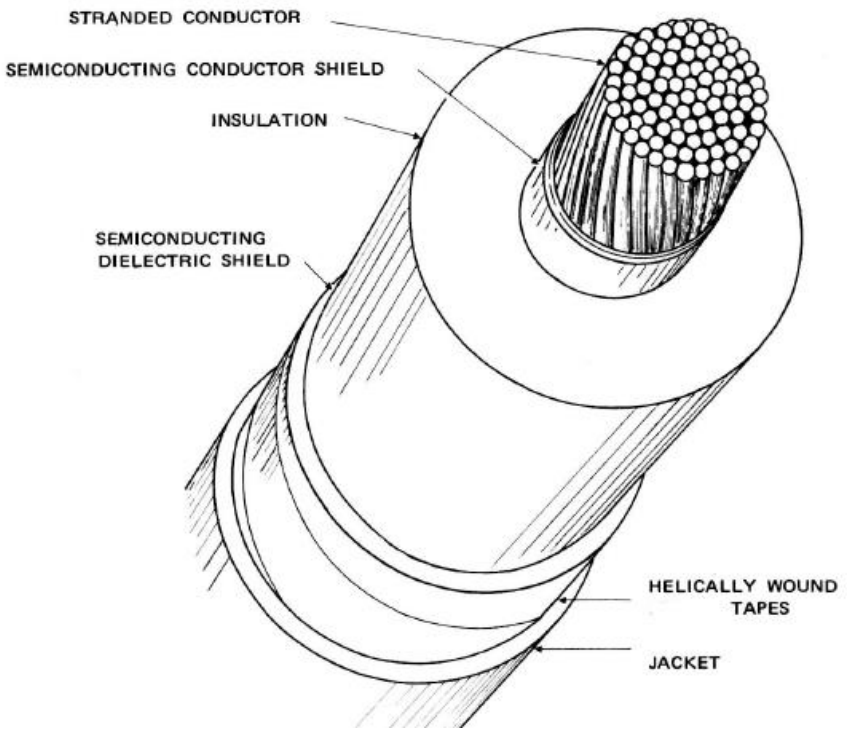

Figure 1: Typical structure of a MV cable [2].

2.2.2 Functional Role of Each Layer

Each layer fulfils a distinct function, playing an important role in ensuring safe and reliable operation. The conductor efficiently transmits electrical current, while being designed to minimize power losses. The cable insulation forms the primary dielectric barrier, capable of withstanding both normal and impulse voltages throughout the cable's lifetime, even under thermal and mechanical stresses caused by electrical loading. The metallic screen prevents external corona from affecting cable performance, stabilizes the internal field and forms an equipotential surface

that eliminates irregularities and protrusions from the previous parts. The metallic screen then serves three purposes, firstly it contains the electric field, safely conducts leakage or earth-fault currents and also acts as a moisture and electromagnetic shield. Finally, the outer sheath functions as the environmental and mechanical shield, protecting the inner layers from water ingress, chemical attack, UV exposure and fire hazards, thereby preserving the cable's electrical integrity throughout its service life [1], [2].

2.2.3 Materials of Cable Components

The performance and reliability of medium voltage cables depend heavily on the materials used for their construction. Each component, from the conductor to the outer jacket, is chosen to meet specific electrical, thermal, and mechanical requirements. Understanding the properties and functions of these materials is essential when evaluating cable behavior under electrical stress [2].

The conductor is typically made of either copper or aluminum, depending on the application. Copper, known for its excellent conductivity and low resistance, is often chosen when efficiency is a priority, despite being heavier and more expensive. For applications requiring the transmission of lower power, where efficiency is not a critical parameter, aluminum conductors are used. Also, in applications where the lighter cable weight is a significant advantage, aluminum is preferred. To improve flexibility and reduce energy losses in alternating current systems, conductors are frequently stranded and not solid [1].

Semiconducting layers are extensively used to create a consistent surface that prevents high electrical stresses on the main insulation. For modern cables with extruded insulation, special semiconducting compounds are used, while traditional paper-insulated cables rely on materials like carbon black or metallized tapes. These materials ensure the cable's safe operation [1].

The insulation layer in MV cables is responsible for electrically isolating the conductor and sustaining the electric field generated during operation. Its dielectric performance is influenced by both chemical and thermal behavior of the insulating material used. According to Table 1, insulating materials are classified into two broad categories: thermoplastic and crosslinked compounds. Thermoplastic materials, such as PVC (polyvinyl chloride), can be softened by heat and reshaped. This limits their application in MV environments due to the material's lower thermal endurance. In contrast, crosslinked compounds, including cross-linked polyethylene (XLPE), ethylene propylene rubber (EPR), and high-modulus EPR (HEPR), undergo a chemical process

that forms a stable three-dimensional molecular network. This structure allows them to retain their shape at elevated temperatures and improves both mechanical integrity and electrical performance of the insulation, under long-term loading and during short-circuit conditions [3], [4].

Table 1: Classification of insulating compounds for MV cables [3].

Insulating compound	**Abbreviated Designation**
a) Thermoplastic polyvinyl chloride intended for cables with rated voltages U_0/U = 3.6/6 kV	PVC/B*
b) Crosslinked:	
ethylene propylene rubber or similar (EPM or EPDM)	*EPR*
high modulus or hard grade ethylene propylene rubber	*HEPR*
cross-linked polyethylene	XLPE

** Insulating compound based on polyvinyl chloride intended for cables with rated voltages $U_0/U \leq 1.8/3$ kV is designated PVC/A in IEC 60502-1.*

Table 2 presents the maximum allowable conductor temperatures for various insulating materials used in power cables. It applies to MV cables rated up to 30 kV nominal voltage and includes polyvinyl chloride (PVC), cross-linked polyethylene (XLPE), and ethylene-propylene rubber types (EPR and HEPR). PVC is limited to 70 °C during normal operation and either 160 °C or 140 °C under short-circuit conditions depending on the conductor's size. Crosslinked materials such as XLPE and EPR offer improved thermal endurance, withstanding up to 90 °C in continuous use and 250 °C for short-circuit events. In addition to thermal stability, polyethylene-based insulations provide additional dielectric characteristics, such as low permittivity, low dielectric losses, and high dielectric strength. XLPE offers enhanced mechanical properties at elevated temperatures and reduced water treeing susceptibility [3], [5].

Table 2: Maximum conductor temperatures for insulating compounds [3].

Insulating Compound	**Maximum Conductor Temperature °C**	
	Normal Operation (°C)	Short-circuit (5 s) (°C)
Polyvinyl chloride (PVC/B) (≤ 300 mm²)	70	160
Polyvinyl chloride (PVC/B) (> 300 mm²)	70	140
Cross-linked polyethylene (XLPE)	90	250
Ethylene propylene rubber (EPR and HEPR)	90	250

A metallic screen, typically made of copper or aluminum tapes or wires, or combinations thereof, is applied over the insulation to provide a low-resistance path for induced and fault currents and to ensure proper grounding. Since the semiconductive layers cannot handle significant fault currents, the metallic screen is essential for directing these safely to earth with a low resistance path and activating protective devices. Therefore, the design must balance mechanical, thermal, and economic factors while ensuring fault current capability. In a few cases, galvanized steel wire or tape armour may also be applied for additional mechanical protection [6], [7].

The outer jacket, also known as oversheath, is a critical component of MV cables, providing mechanical protection, environmental sealing, and resistance to external stresses such as UV radiation, chemical exposure, and abrasion. While the terms sheath and jacket are often used interchangeably, they refer to distinct parts of the cable. Jacket selection must consider various factors such as expected temperature range, mechanical handling, moisture exposure, flame resistance, and ease of installation.

Polyvinyl chloride (PVC) is one of the most common thermoplastic jacket materials. According to Table 3, PVC jackets are classified under two standard types: ST1 and ST2, as defined by IEC standards. These designations refer to the thermal performance and environmental resistance of the material. ST1 is suitable for cables with a maximum conductor operating temperature of 80 °C, while ST2 supports up to 90 °C, offering improved resistance to heat and deformation. These classifications are shown in Table 4, which details allowable operating conditions for both PVC and polyethylene (PE). PVC offers flame resistance and adequate strength,

but it has limitations in moisture resistance and tends to deform under continuous pressure or high temperatures [5].

Polyethylene (PE) is often selected for its superior moisture resistance and long-term aging stability. PE jackets are designated as ST3 and ST7, with temperature ratings of 80 °C and 90 °C, as shown in both Table 3 and Table 4. PE is available in low-density (LDPE), medium-density (MDPE), and high-density (HDPE) forms. LDPE is valued for flexibility, while HDPE is used for ruggedized jackets due to its mechanical toughness. PE is typically black and compounded with 2,5–3,0% carbon black to improve UV resistance [5].

Elastomeric compounds, such as polychloroprene (CR) and chlorosulfonated polyethylene (CSPE), are classified under the SE_1 category in Table 3, with an operating temperature of 85 °C. These materials are used when greater flexibility, oil resistance, or thermal stability is required. They retain flexibility at low temperatures and outperform PVC in chemically aggressive or high-heat environments [5].

Table 3: Maximum conductor temperatures for different types of sheathing compound [3].

Sheathing compound	**Abbreviated designation**	**Maximum conductor temperature in normal operation °C**
a) Thermoplastic polyvinyl chloride (PVC)	ST1 ST2	80 90
polyethylene	ST3 ST7	80 90
b) Elastomeric: polychloroprene, chlorosulfonated polyethylene or similar polymers	SE1	85

Table 4: Oversheathing compounds for cables [4].

Oversheathing compound	**Abbreviated designation**	**Maximum conductor temperature in normal operation °C**
Polyvinyl chloride (PVC)	ST1 ST2	80 90
Polyethylene	ST3 ST7	80 90

2.3 Dielectric Strength and Electrical Breakdown in Cable Systems

Dielectric strength is the material's ability to withstand electric stress without leading to insulation failure. The dielectric strength of the material defines the voltage limit to electrical breakdown. Understanding these mechanisms is essential for predicting cable lifespan and ensuring safe, reliable operation under real-world conditions. In cable systems, electrical breakdown refers to the catastrophic failure of an insulating material when subjected to an electric field beyond its dielectric strength. This process causes a sudden increase in current and a drop in voltage across the cable, often tripping protective devices such as circuit breakers. While breakdown can occur abruptly, its onset is typically linked to underlying degradation mechanisms or structural defects within the insulation [8].

2.3.1 Definition of Dielectric Strength

Dielectric strength is defined as the voltage gradient at which dielectric failure of the insulating material occurs under specific conditions or test. According to ASTM D149, the terms 'dielectric strength' and 'electric strength' are used interchangeably. So, electric strength tests measure the ability of insulating materials to resist electrical breakdown when subjected to high voltage. The materials, despite having high electric strength, while subjected to heated, humid or deteriorated environments, might lack performance [9], [10].

2.3.2 Electrical Breakdown Mechanisms

One of the primary contributors to breakdown in cable insulation and jacket is partial discharge, a localized electrical discharge that does not completely cross the insulation. These discharges typically result from high local electric field concentrations within voids, at interfaces, or along the surface of the insulation. Partial discharge often appears as short-duration pulses, generally lasting less than one microsecond, though continuous or pulse-less forms can also arise, especially in gaseous dielectrics. These events release energy in the form of light, heat, sound, and chemical reactions, progressively damaging the insulation. In cable systems, persistent partial discharge activity is a key precursor to long-term insulation degradation and eventual breakdown [11].

A subcategory of partial discharges are surface discharges, which are localized partial discharges that occur along the surface of insulation or jacket, typically due to moisture, dirt, or surface defects. Over time, they can deteriorate the material and form conductive tracking paths,

increasing the risk of full discharge. This type of discharge is often found in aged cable terminations or contaminated outer jackets [8].

Another long-term failure process affecting polymer-insulated cables is water treeing. This phenomenon develops when moisture infiltrates the insulation, either through the outer jacket or via imperfections near the conductor screen. Water trees reduce the AC and impulse breakdown strengths of a cable. They usually grow much more slowly than electrical trees. Cable failure typically occurs during, or as a result of, switching operations or lightning impulse surges, especially when an electrical tree initiates at the tip of a large water tree [1].

2.3.3 Aging and Degradation

The durability of MV cable systems depends on the long-term integrity of both the main insulation and the outer protective jacket. These components are continuously exposed to a variety of electrical, thermal, mechanical, and environmental stresses that contribute to their gradual aging. Over time, such stresses can initiate physical, chemical, or electrical deterioration, compromising the cable's dielectric strength and leading to potential breakdown [1].

To visualize the complexity of these mechanisms, Figure 2**,** Figure 3 and Figure 4 present conceptual flow diagrams of insulation system failure under different stress conditions. Each Figure outlines how contaminants, manufacturing defects, or improper handling can interact with electrical stress, elevated temperatures, or environmental exposure, ultimately resulting in degradation phenomena such as partial discharge, water treeing, thermal aging, or loss of mechanical strength. These stress pathways often act simultaneously, creating a synergistic effect that accelerates material aging [8].

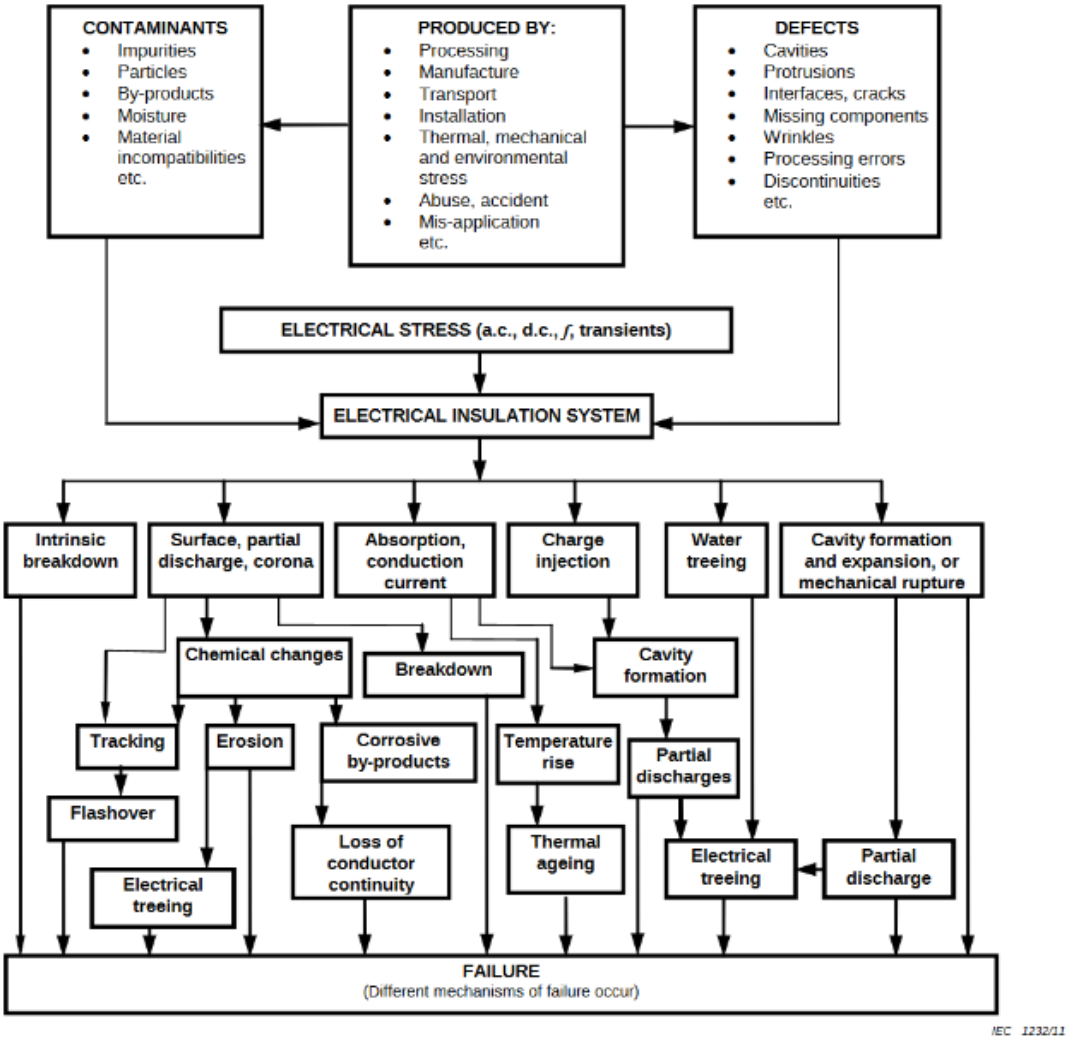

Figure 2: Failure mechanisms in cable insulation systems under electrical, thermal, and environmental stress [8].

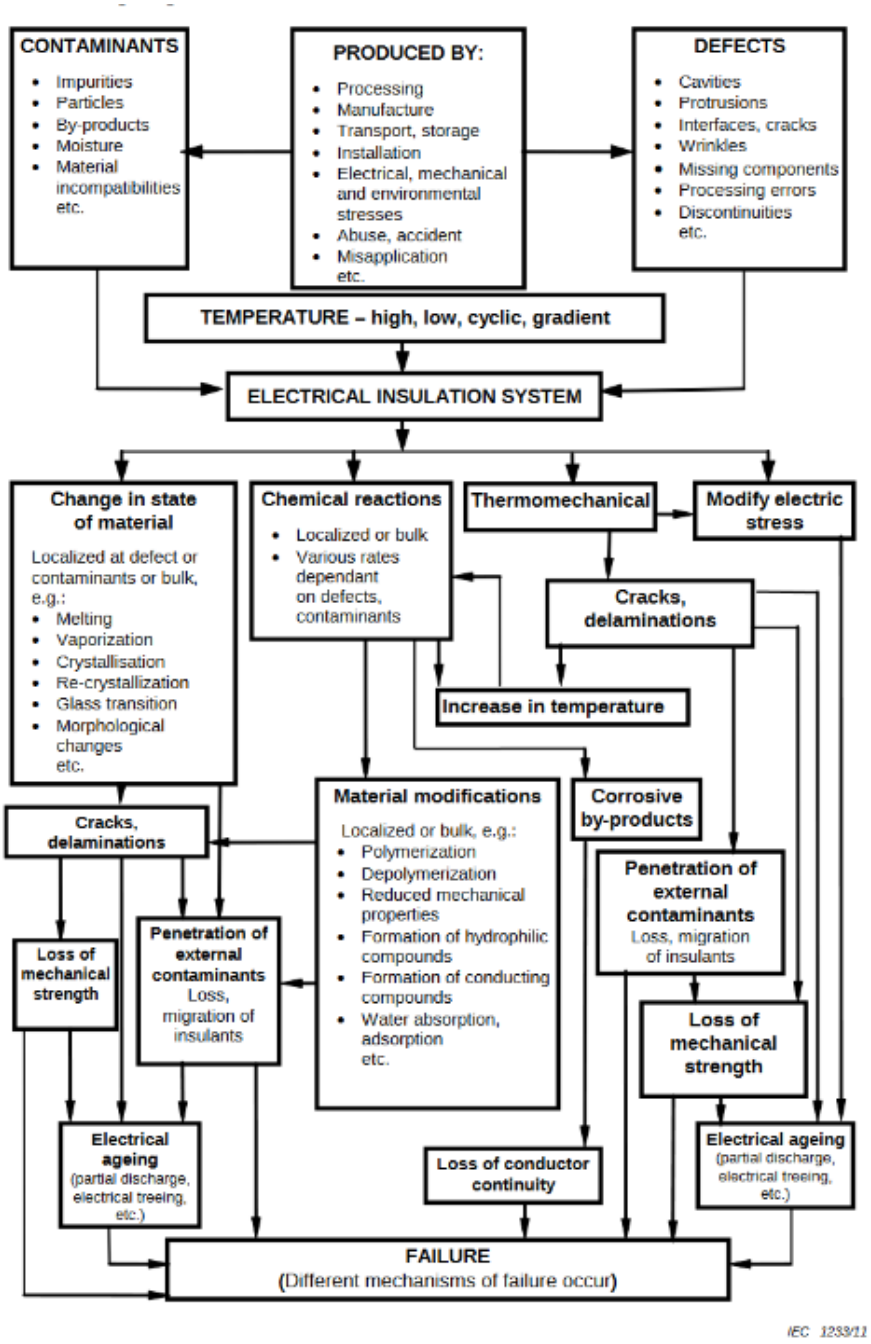

Figure 3: Failure mechanisms in cable insulation systems under electrical, thermal, and environmental stress [8].

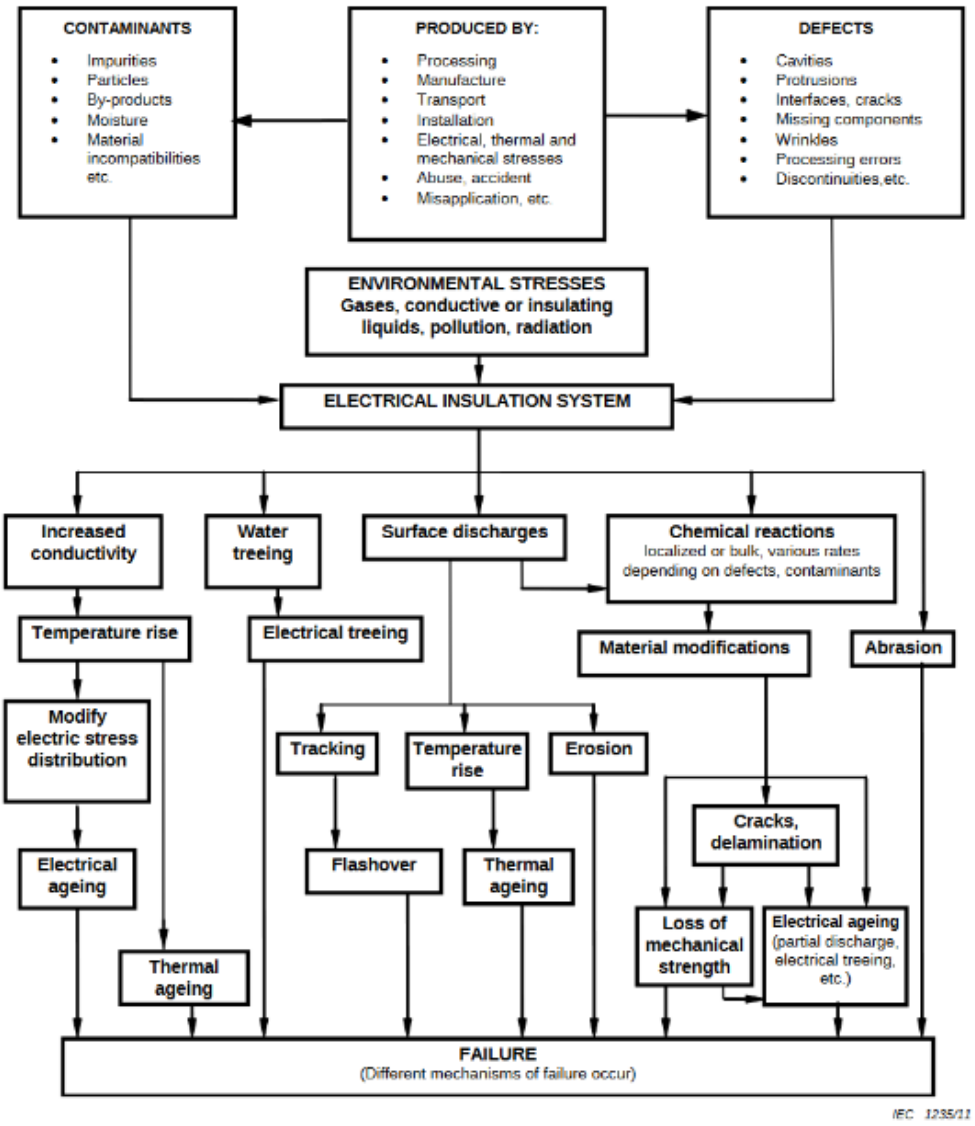

Figure 4: Failure mechanisms in cable insulation systems under electrical, thermal, and environmental stress [8].

2.4 Cable Testing

Standards outline testing procedures and define tests to evaluate and verify the cable's design and production, while, in some cases, test the cable's behavior to special conditions. Each test evaluates specific aspects of cable integrity under defined conditions, providing insight into the material's dielectric behavior, mechanical resilience, and resistance to environmental stress.

2.4.1 Classification of Tests

In accordance with IEC standards for medium and medium-to-high voltage cables, the testing procedures primarily apply to single-core cables and their integral components under standard installation and operating conditions, while transition joints and accessories are addressed separately and not considered within the scope of these core cable tests. Both of these cable types, operating from 1 kV (Um = 1,2 kV) up to 30 kV (Um = 36 kV), as well as cables that cover the spectrum above 30 kV up to 150 kV (Um = 170 kV), comply with a variety of tests to ensure their performance in high-voltage environments. In fact, they share a significant alignment when it comes to testing conditions and testing methods overall [3], [4].

These tests are conducted under controlled environmental conditions, where temperature and humidity are regulated to ensure consistent results. For AC voltage tests, the frequency of the applied voltage is maintained between 49 Hz and 61 Hz, with a purely sinusoidal waveform. The testing is performed at a room temperature of 20 ± 15 °C, in accordance with IEC guidelines [3], [4].

When impulse voltages are applied, during lightning impulse testing, the shape and timing of the waveform must conform to internationally accepted specifications. In accordance with IEC 60230, the impulse voltage shall exhibit a virtual front time between 1 μs and 5 μs, and a nominal time to half-value (tail time) between 40 μs and 60 μs. In all other respects, the waveform shall comply with the requirements defined in IEC 60060-1, ensuring consistency, reproducibility, and compatibility with standard high voltage testing methodologies [3], [4], [12], [13].

Medium and medium-to-high voltage cable tests are similar in their methodologies and objectives, ensuring performance and safety under designated conditions. However, there are some differences in the specific requirements and applications due to the lower voltage range of MV cables. Specifically, the tests are categorized in the following format:

- **Routine tests:** Mandatory tests performed by the manufacturer to ensure that every length of the cable meets the required criteria.
- **Type tests:** Type tests are crucial for the validation of the design, manufacturing process and materials of the cables as they serve as a comprehensive assessment to verify that the cable design meets the required standards. Once these tests are

successfully completed, they do not need to be repeated unless there are changes to the cable or its accessories, such as modifications in materials, manufacturing processes, design, or electrical stress levels, that could negatively impact performance.

- **Prequalification tests:** Prequalification tests are needed only if there has been a manufacture or design change in the cable system and are conducted by placing an already prequalified part in the system. These tests typically involve heating cycles, lightning impulse voltage tests, and examinations. However, in medium voltage cable systems smaller samples are required, reflecting the reduced operational stress compared to higher voltage systems.

- **Tests after installation:** Tests after installation are carried out when the installation of the cable and its accessories has been completed.

2.4.2 Insulation Testing

Cable technology-oriented standards and textbooks have established a range of tests specifically designed to assess the dielectric strength of cable insulation under defined conditions. These tests evaluate the insulation's ability to withstand electrical stress during nominal operation and transient events without failure, providing essential data on material integrity and long-term reliability.

More specifically, as outlined in ASTM D149-09, the test involves applying an alternating voltage, typically at a standard frequency of 60 Hz, as the standard refers to US, to an insulating material sample. The voltage amplitude starts at zero, or a value significantly below the expected breakdown voltage, and is increased until the material fails. The test is conducted using simple electrodes positioned on opposite sides of the material, which may be molded, cast, or cut from sheets or plates. Alternative electrode and sample arrangements can be used to fit the material's shape or replicate conditions for a specific application, ensuring a comprehensive evaluation of the material's electrical insulating capabilities [9].

Different standards, such as those established by IEC and IEEE, emphasize the importance of insulation strength and specify comprehensive testing protocols. Although many of these tests assess the cable as a whole, certain tests specifically target the evaluation of the main insulation

itself. These procedures, applicable to both medium and high voltage cables, are typically categorized into:

- **Routine tests**

Voltage withstand test: Being one of the most basic tests on cable insulation, voltage withstand test involves applying either a nominal or an elevated voltage to the cable for a prescribed period. It ensures the insulation's ability to withstand operational stress without breakdown. Simple withstand tests provide pass/fail results, whereas monitored withstand tests analyze additional attributes, such as partial discharge or dielectric response, for more detailed insights [14].

- **Type tests**

1. Partial discharge test: This test is essential for assessing the quality and reliability of a cable's insulation by measuring the charge of small, localized electrical discharges that occur within the insulation. These discharges are often caused by hidden flaws, voids, or defects in the material, which can gradually weaken the insulation over time. The test process involves applying a controlled voltage between the conductor and the screen, starting with a gradual increase to 1.75 times the rated voltage (U_0). This voltage is held for 10 seconds and then reduced to 1.5 U_0, ensuring that no partial discharges exceed a sensitivity limit of 5 picocoulombs (pC) [4].

To mimic real-world operating conditions, the test can also be performed at elevated temperatures. In such cases, the cable is heated to 5–10 K above its usual maximum operating temperature using conductor current and maintained at this level for at least two hours. If the desired temperature cannot be achieved, additional thermal insulation can be used. This procedure not only ensures the insulation can withstand everyday stresses but also helps uncover any potential defects that might impact its long-term performance. By focusing on issues like voids, surface discharges, and corona effects, partial discharge measurements offer valuable insights into the insulation's durability and reliability, contributing to the safe and efficient operation of the cable [4], [15].

The partial discharge testing is further enhanced by the identification of partial discharge inception voltage (PDIV) and extinction voltage (PDEV), which define the voltage levels at which partial discharges begin and cease. The test is applicable for both AC and DC voltages, making it

useful for a wide range of high-voltage applications and also contributing to the efficient operation of high-voltage cable [16], [15].

2. Heating cycle voltage test: In this test, the conductor is heated and cooled through repeated cycles to simulate operational temperature fluctuations. Simultaneously, voltage of $2U_0$, is applied, while the conductor reaches its maximum rated temperature. To pass, the insulation must show no signs of breakdown [4].

3. Tan δ measurement: In this test, the cable is heated by running current through its conductor until it reaches 5 to 10 degrees above its normal operating temperature. The temperature is monitored using resistance measurements or temperature sensors placed on the sheath or another identical sample. If the target temperature is not reached, additional insulation can be applied. Once heated, the dielectric loss (tan δ) is measured to ensure it stays within the acceptable limits defined by the standards [4].

Table 5: Tan δ per material [4].

Designation of Compound	**PE**	**HDPE**	**EPR/HEPR**	**XLPE**
Maximum tan δ (× 10⁻⁴.)	10	10	50	10[a]

[a] *For cables produced with an XLPE compound containing special additives, the maximum tan δ is 50 × 10⁻⁴.*

4. Lightning impulse voltage test followed by a power frequency voltage test: In this test, first, a lighting impulse test is conducted. The test involves a structured application of impulses. It begins with 10 negative impulses at a specific voltage, followed by 5 positive impulses starting at half that voltage and gradually increasing to 85% of the initial value. This is repeated with alternating sequences of 10 positive and negative impulses at various voltage levels. The test progresses systematically, ensuring the cables can handle voltages both within and beyond their specified limits. For the test to be considered valid, the assembly should remain intact for 10 positive and 10 negative impulses. After that, the assembly should be subjected to a power frequency voltage test with magnitude of $2U_0$. The test is successful as long as there is no breakdown or flashover [17].

5.Impulse dielectric strength test: It measures the dielectric breakdown voltage of solid insulating materials under impulse voltage conditions. The test applies a 1,2/50 μs full-wave

impulse, simulating the effects of lightning surges and switching transients in high-voltage equipment. By exposing insulation to these fast-rising, high-energy pulses, the test evaluates its ability to withstand sudden electrical stress without breakdown [4].

- **Tests after installation**

AC voltage test on insulation: After installation, an AC voltage test is conducted to ensure the insulation remains intact and uncompromised by transportation, handling, or installation procedures. This test involves applying a sinusoidal alternating current voltage. The test parameters—voltage magnitude and duration—are determined based on the specific application and system rating. As an alternative, a continuous test at rated voltage (U_0) may be performed for 24 hours. These post-installation tests are essential for verifying that the cable is safe to energize and that the insulation has not been mechanically or electrically damaged [18].

Table 6 summarizes the standard voltage levels applied during key dielectric tests for various rated voltage classes of medium and high-voltage cables. These tests are essential for verifying the insulation performance and long-term reliability of cable systems under both factory and field conditions, in accordance with relevant international standards [4].

Table 6: Rated voltages per test [4].

1	2	3	4	5	6	7	8
Rated Voltage (U) (kV)	**Highest Voltage for Equipment (U_m) (kV)**	**Value of U_0 (kV)**	**Partial Discharge Test (1.5 U_0) (kV)**	**Tan δ Measurement (U_0) (kV)**	**Heating Cycle Voltage Test (2 U_0) (kV)**	**Lightning Impulse Test (kV)**	**Voltage Test after Installation (kV)**
45 to 47	52	26	39	26	52	250	52
60 to 69	72,5	36	54	36	72	325	72
110 to 115	123	64	96	64	128	550	128
132 to 138	145	76	114	76	152	650	132
150 to 161	170	87	131	87	174	750	150

2.4.3 Cable Jacket Testing

There are tests that solely focus on the jacket of the electric cable and the tests that they must undergo to certify their operation. Whether the system is insulated or not, the tests are categorized into three big categories:

- **Routine tests**

1.Electrical test on cable jacket: This test is performed to evaluate the dielectric integrity of the cable's outer sheath under simulated service conditions. In this procedure, the middle portion of the cable sample is fully immersed at ambient temperature in a conductive solution consisting of 0,5% sodium chloride by weight in water, with the addition of approximately 0,1% by weight of a suitable non-ionic surface active agent. This conditioning phase lasts for at least 24 hours, ensuring sufficient moisture ingress and exposure of the jacket to a conductive medium.

Following immersion, a direct current (DC) voltage of 20 kV is applied for one minute between the metallic layer beneath the jacket and the surrounding saline solution. The underlying metal conductor is held at negative polarity. This step is designed to detect any conductive paths or breakdown points through the jacket that may form under high-voltage DC stress in the presence of moisture and ionic contamination.

While the cable remains submerged, the test continues with the application of standard lightning impulse voltages, as defined in IEC 60230. A total of twenty impulses is applied, ten positive and ten negative, representing typical overvoltage conditions such as those caused by switching events or lightning strikes. The magnitude of the applied impulse voltage depends on the rated lightning impulse withstand level of the main insulation of the cable and is selected in accordance with Table 7. Peak impulse test voltages range from 30 kV for cables rated up to 325 kV, to 72,5 kV for cables rated above 1550 kV [12].

This combination of DC and impulse testing under saline conditions is intended to simulate severe field environments and verify that the outer sheath provides adequate dielectric protection and environmental sealing. The procedure ensures that the jacket can prevent moisture penetration and electrical tracking, even under elevated voltage stress and in the presence of conductive contaminants [18].

Table 7:Impulse test voltage [18].

Rated lightning impulse withstand voltage of main insulation voltage (peak) kV	**Impulse test voltage (peak) kV**
$V \leq 325$	30
$325 < V \leq 750$	37,5
$750 < V < 1175$	47,5
$1\,175 \leq V < 1550$	62,5
$V \geq 1550$	72,5

2.Spark test: During the test, the cable is passed through an energized electrode that applies a high voltage, with the inner metal layer grounded for A.C. or connecting it to the negative pole for D.C. Voltages should be around 6 kV A.C. per mm capped at 15 kV or 9 kV D.C. per mm capped at 25 kV. It is specifically limited to layers up to 2.0 mm thick and not applicable for insulation rated above 3 kV. The spark test is used to detect weaknesses in the insulation or sheath of a cable [18], [19].

- **Type tests**

1. Bending test on the cable: This test's scope is to examine the stress a cable may face by bending it around a cylinder to check for permanent damage or deformation [4].

2. Abrasion test: The abrasion test's purpose is to show that oversheath can tolerate abrasion while being laid. First, before testing, the cable sample is bent is bent complying with the corresponding IEC bending description. Then, the test procedure requires the bent cable to be laid flat and straight on a solid surface, with the bending plane horizontal. Then, a steel bar with a rounded edge is placed across the middle of the cable, vertically to its length. This bar is weighed down with a force that depends on the cable's diameter. The weighed bar is dragged back and forth along a 600 mm section of the cable at a controlled speed (150 – 300 mm per second). This motion is repeated 50 times, with 25 passes in one direction and 25 in the opposite direction. After the abrasion process, the jacket is examined for any visible damage and the abraded section is

immersed in a saline solution and subjected to a 20 kV voltage to ensure that the jacket still provides insulation [18].

- **Tests after installation**

DC Voltage Test: After installation, the cable oversheath should be tested using a DC voltage of 4 kV per mm of its thickness, up to a maximum of 10 kV DC. This voltage is applied between the metallic layers beneath the jacket and an outer electrode for 1 minute. The test is considered successful if there is no breakdown on the jacket [18].

2.4.4 Overview of Standards and Testing Methods

Table 8 and Table 9 present a concise overview of the electrical tests performed on both the insulation and jacket of medium and medium-to-high-voltage cables. Each table includes only tests that involve the application of electrical stress, whether AC, DC, or impulse voltage.

Table 8: Insulation electrical tests overview.

TEST NAME	**STANDARD**	**TEST DESCRIPTION**
Voltage Withstand Test	IEEE STD 400	The test involves immersing the cable in a saline solution and subjecting it to both a 20 kV DC voltage and standardized lightning impulse voltages.
Partial Discharge Test	IEC 60840	Ensures no discharges exceed 10 pC for cables and 5 pC for accessories. Voltage is applied at 1.75U_0 for 10 seconds, then reduced to 1.5U_0.
Heating Cycle Voltage Test	IEC 60840	Simulates operational conditions by applying 2U_0 during repeated heating/cooling cycles to check insulation durability.
Tan δ Measurement	IEC 60840	Conducted at elevated temperatures (5–10 K above operating conditions) to ensure dielectric loss remains within limits.
Lightning Impulse Voltage Test	IEC 60230, IEC 60840	Cable is subjected to a 1,2/50 μs impulse (10 pos. + 10 neg. waves)
Power Frequency Voltage Test	IEC 60840	Power frequency voltage at 2U_0 is applied to ensure no breakdown or flashover.
Impulse Dielectric Strength Test	IEC 60840	Measures dielectric breakdown voltage of solid insulating materials using 1,2/50 μs full-wave impulses. Simulates lightning surges in high-voltage equipment.
AC Voltage Test	IEC 60840	Applies a DC voltage of 4 kV per mm of oversheath thickness, up to a maximum of 10 kV, for 1 minute to detect any insulation breakdown.

Table 9: Jacket electrical tests overview.

TEST NAME	**STANDARD**	**TEST DESCRIPTION**
Electrical Test on Oversheath	IEC 60229	Upon request, to verify outer jacket integrity and absence of cracks or damage.
DC Voltage Test	IEC 60229	A DC voltage of 4 kV per mm of oversheath thickness (up to 10 kV) is applied for 1 minute to detect faults in manufacturing.
Spark Test	IEC 62230	Detects insulation weaknesses by applying 6 kV AC per mm of oversheath thickness (up to 15 kV) or 9 kV DC per mm (up to 25 kV).
Bending Test	IEC 60840	Evaluates mechanical stress by bending the cable around a cylinder to check for permanent deformation or damage.
DC Voltage Test	IEC 60229, IEC 60840	Applies a DC voltage of 4 kV per mm of oversheath thickness, up to a maximum of 10 kV, for 1 minute to detect any insulation breakdown.

CHAPTER 3: EXPERIMENTAL SETUP AND METHODOLOGY

3.1 Introduction

The chapter presents the process of evaluating the dielectric strength of various medium voltage cable samples when subjected to high voltage impulse conditions. First, the experimental and measuring equipment utilized in the study is detailed and then the specific types of medium voltage cables examined are listed. Subsequently, the experimental methodology is then systematically presented, followed by a detailed description of the test environment and setup configuration. Ultimately, the results obtained are thoroughly analyzed and evaluated.

3.2 Cable Samples and Characteristics

This study examines five distinct types of MV cable samples. Each cable type serves a different purpose due to variations in morphology or material selection in order to meet specific electrical, mechanical and environmental requirements. The structural differences among these cables, circulating around conductor type, insulation material and oversheath, directly affect their operational limits and performance. Due to the uneven cable geometry caused by the underlying wire screen deformation, the outer sheaths do not maintain a uniform thickness along the cable's circumference. To calculate the actual jacket thickness of each cable type, ten individual measurements were taken from two separate samples using a digital caliper at equally spaced positions around the cable. The average of these measurements was used as the representative jacket thickness for each type.

3.2.1 Cable Type A: NA2XSY 20kV, CWS, PVC

Cable Type A is a single-core medium voltage cable, rated for operation at 20 kV. The cable's manufacturing conforms to the German technical standard VDE 0276 that focuses on cables with extruded insulation used in power distribution systems. Its design is optimized for deployment in pipes or cable ducts, directly in-ground, or in free air [20].

Construction and Materials

The cable consists of a stranded aluminum conductor, which provides a lightweight and cost-effective solution compared to copper, with a nominal cross-sectional area of 50 mm^2. Surrounding the conductor is an inner semiconductive layer providing even electric field distribution. The insulation layer is composed of cross-linked polyethylene (XLPE), selected for its high dielectric strength and thermal resistance. Over the insulation, an outer semiconductive layer, complemented by a small layer of fabric, ensure proper bonding with the metallic components. The cable includes a copper wire screen (CWS) and also a stranded copper tape screen. Prior to jacket application, a paper wrap layer is incorporated to smooth out surface irregularities and prevent galvanic interaction between the metallic screens and protective layers. Externally, a polyvinyl chloride (PVC) cable jacket offers protection against external factors.

Jacket Thickness Measurement

To determine the representative jacket thickness of cable Type A, ten measurements were taken from two different samples.

Table 10: Jacket thickness measurements (in mm) for two samples of cable Type A.

Jacket Thickness (mm)	1	2	3	4	5	6	7	8	9	10
Sample 1	**2,20**	**2,25**	**2,28**	**2,30**	**2,24**	**2,17**	**2,31**	**2,26**	**2,19**	**2,34**
Sample 2	**2,23**	**2,32**	**2,22**	**2,35**	**2,18**	**2,29**	**2,21**	**2,35**	**2,24**	**2,26**

Calculated average of sample 1: 2,254 mm → 2,3 mm

Calculated average of sample 2: 2,3 mm → 2,3 mm

Calculated Type B jacket thickness average: 2,2595 mm → 2,3 mm

For NA2XSY cables with a nominal voltage rating of 20 kV and a conductor cross-sectional area of 50 mm², the VDE 0276 standard specifies a nominal outer sheath thickness of 1,8 mm. However, based on the experimental measurements performed on the available samples, the calculated average jacket thickness was found to be 23 mm. This difference may be attributed to

manufacturing variations, additional extrusion tolerance, or enhancements made by the manufacturer for improved mechanical protection. Therefore, in this thesis, the experimentally determined jacket thickness of 2,3 mm is adopted for further analysis.

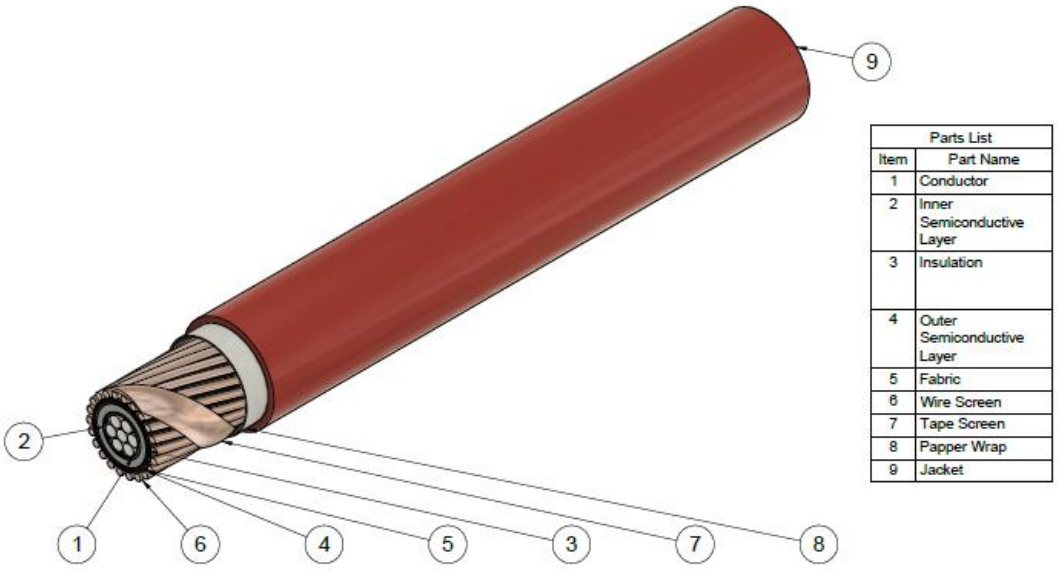

Parts List	
Item	Part Name
1	Conductor
2	Inner Semiconductive Layer
3	Insulation
4	Outer Semiconductive Layer
5	Fabric
6	Wire Screen
7	Tape Screen
8	Papper Wrap
9	Jacket

Figure 5: 3D model of Cable Type A with numbered structural layers and parts list.

Figure 6:Photographs of the actual Cable A sample used in the experimental setup: (left) side view of the cable segment with partially stripped outer sheath, and (right) cross-sectional view showing the conductor bundle, insulation, and exposed screen layers.

3.2.2 Cable Type B: 20kV, CWS, PPS+HDPE

Cable Type B is a single-core medium voltage cable rated for continuous operation at 20 kV. The structural design and material selection suggest that this cable is intended for medium voltage power distribution in demanding industrial environments.

Construction and Materials

The cable features a 150 mm^2 stranded copper conductor. Surrounding the conductor, an inner semiconductive layer establishes mechanical separation between the cable's components. The main insulation consists of cross-linked polyethylene (XLPE) due to its excellent dielectric properties. Over the insulation lies an outer semiconductive layer as well as a layer of fabric, co-extruded to maintain contact with the insulation and facilitate bonding to the metallic screen layers. The cable includes a copper wire screen (CWS) and also a stranded copper tape screen. To ensure a uniform surface and eliminate electrochemical reactions, a white thermoplastic interlayer is installed over the metallic screens before jacketing. A dual-layer composite sheath, made from high-density polyethylene (HDPE) and polyphenylene sulfide (PPS) protects the cable from external damage. PPS is a high-performance thermoplastic known for its robustness and exceptional resistance to heat. When combined with HDPE, the material pairing is suitable for harsh environments.

Jacket Thickness Measurement

To determine the representative jacket thickness of cable Type B, ten measurements were taken from two different samples.

Table 11: Jacket thickness measurements (in mm) for two samples of cable Type B.

Jacket Thickness (mm)	1	2	3	4	5	6	7	8	9	10
Sample 1	**2,65**	**2,55**	**2,52**	**2,50**	**2,33**	**2,47**	**2,47**	**2,45**	**2,50**	**2,32**
Sample 2	**2,47**	**2,36**	**2,31**	**2,41**	**2,48**	**2,50**	**2,45**	**2,35**	**2,55**	**2,35**

Calculated average of sample 1: 2,476 mm → 2,5 mm

Calculated average of sample 2: 2,423 mm → 2,4 mm

Calculated Type B jacket thickness average: 2,4495 mm → 2,4 mm

The rounded calculated average jacket thickness of each sample was 2,5 mm and 2,4 mm, respectively, yielding an overall average of 2,4 mm. This value will be considered as the actual jacket thickness of Cable Type B for the purposes of analysis throughout this study.

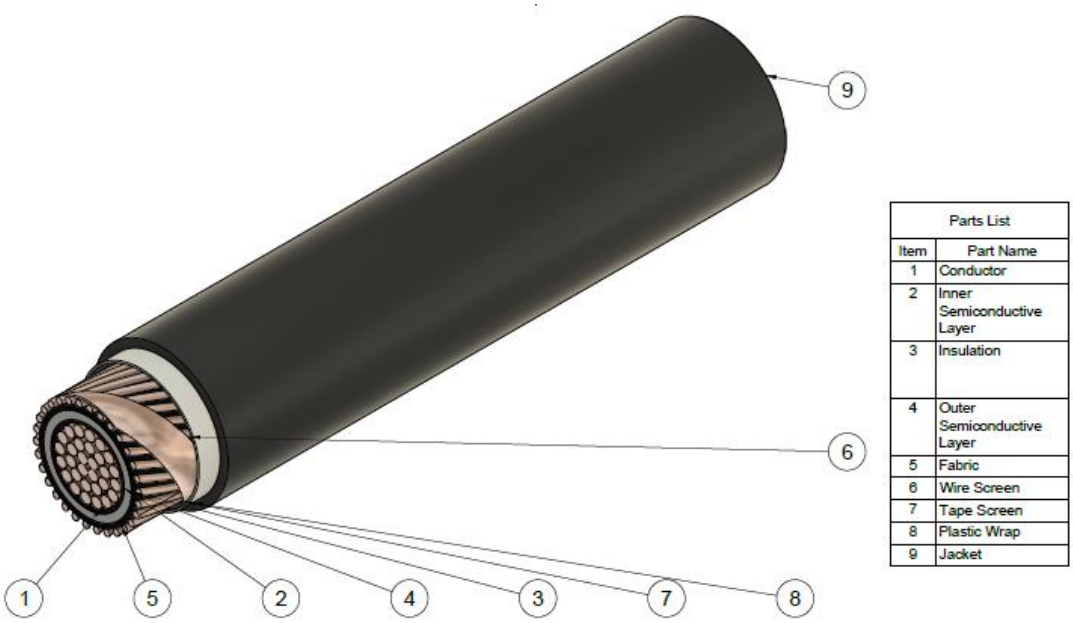

Parts List	
Item	Part Name
1	Conductor
2	Inner Semiconductive Layer
3	Insulation
4	Outer Semiconductive Layer
5	Fabric
6	Wire Screen
7	Tape Screen
8	Plastic Wrap
9	Jacket

Figure 7: 3D model of Cable Type B with numbered structural layers and parts list.

Figure 8: Photographs of the actual Cable B sample used in the experimental setup: (left) side view of the cable segment with partially stripped outer sheath, and (right) cross-sectional view showing the conductor bundle, insulation, and exposed screen layers.

3.2.3 Cable Type C: 20kV, AL-PE, HDPE

Cable Type C is a single-core medium voltage power cable rated for continuous operation at 20 kV. Its configurations and material composition indicate suitability for industrial or utility-scale power networks, especially in locations where mechanical integrity and environmental resistance are critical.

Construction and Materials

At the core of the cable lies a stranded aluminum conductor with a nominal cross-sectional area of 185 mm², selected to reduce weight and installation cost while maintaining acceptable conductivity. This conductor is encased by a semi-conducting layer to smoothen the electric field distribution and minimize localized electrical stress. The main insulating layer consists of cross-linked polyethylene (XLPE), providing thermal stability and high insulation resistance. A second semiconducting layer is extruded over the insulation, bonded with an interface fabric to ensure close contact between internal layers and promote adherence with the metallic screen components. An aluminum concentric neutral system encircles the insulation shield, acting both as an

equipotential layer and as a return path for fault currents. To separate the metallic screen from the external sheath, a non-conductive buffer layer is applied, preventing unwanted interactions. The cable jacket is made from high-density polyethylene (HDPE), a material chosen for its toughness, chemical resistance, and resistance to water ingress. This ensures long-term durability, particularly when installed in moist or chemically active soils.

Jacket Thickness Measurement

To evaluate the effective jacket thickness of Cable Type C, ten circumferential measurements were performed on each of two separate cable pieces

Table 12: Jacket thickness measurements (in mm) for two samples of cable Type C.

Jacket Thickness (mm)	1	2	3	4	5	6	7	8	9	10
Sample 1	**2,64**	**2,66**	**2,38**	**2,59**	**2,67**	**2,61**	**2,42**	**2,47**	**2,69**	**2,56**
Sample 2	**2,39**	**2,46**	**2,53**	**2,41**	**2,52**	**2,63**	**2,34**	**2,48**	**2,66**	**2,41**

Calculated average of sample 1: 2,569 mm → 2,6 mm

Calculated average of sample 2: 2,484 mm → 2,5 mm

Calculated Type B jacket thickness average: 2,5256 mm → 2,5 mm

The rounded calculated average jacket thickness of each sample was 2,6 mm and 2,5 mm, respectively, yielding an overall average of 2,5 mm. This value will be considered as the actual jacket thickness of Cable Type C for the purposes of analysis throughout this study.

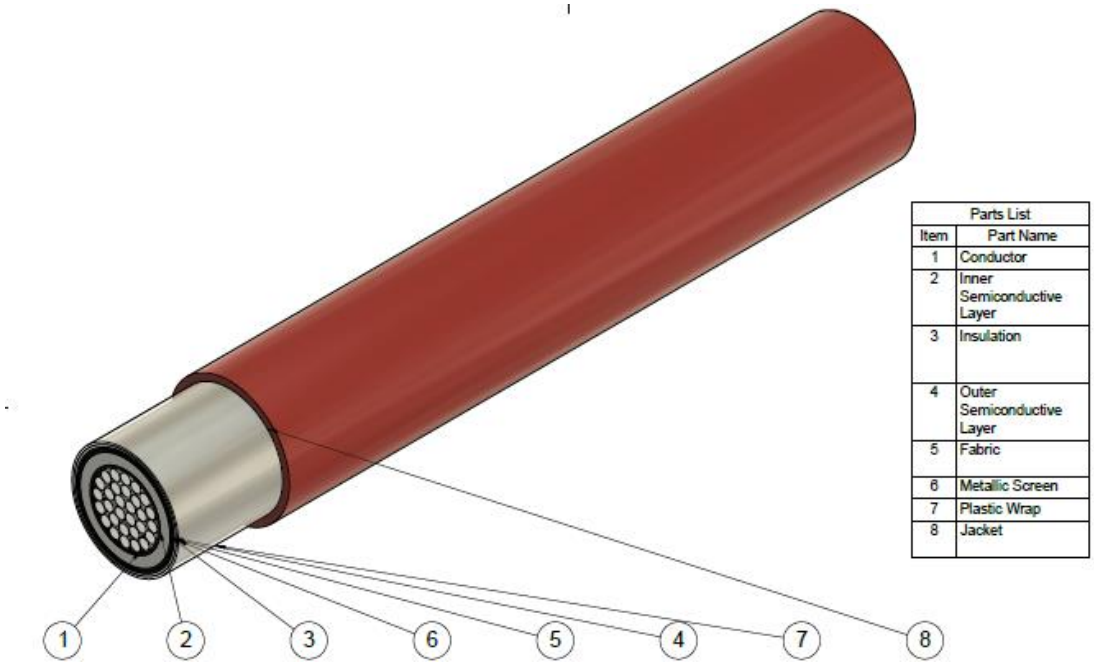

Figure 9: 3D model of Cable Type C with numbered structural layers and parts list.

Figure 10: Photographs of the actual Cable C sample used in the experimental setup: (left) side view of the cable segment with partially stripped outer sheath, and (right) cross-sectional view showing the conductor bundle, insulation, and exposed screen layers.

3.2.4 Cable Type D: 20kV, AL-PE, MDPE

Cable Type D represents a single-core medium voltage cable, engineered for power transmission at a rated voltage of 20 kV and designed conforming to IEC 60502-2. This international standard emphasizes construction, dimensions and test requirements of power cables with extruded solid insulation from 6 kV up to 30 kV for fixed installations. This type of cable is widely employed in power distribution networks and across various industrial sectors.

Construction and Materials

The conductor configuration employs stranded aluminum wires with a nominal cross-section of 120 mm². Surrounding the conductor is an inner semiconductive layer, providing a physical interface that isolates the conductor from the surrounding insulation layers. The main insulation layer consists of cross-linked polyethylene (XLPE), chosen for its excellent dielectric strength and thermal stability. Over the insulation, an outer semiconductive layer is applied to facilitate bonding with the surrounding screen. In addition, a layer of fabric is included, acting as a mechanical buffer that aids in the integration of the metallic screen. Incorporated lies a metallic screen composed of aluminum-polymer laminate (AL-PE), protecting the cable's core from physical damage while shielding it against electromagnetic interference. To isolate the screen from the jacket and avoid surface irregularities, a plastic wrapping layer is applied. The cable is shielded with a medium-density polyethylene (MDPE) outer sheath, which serves as the jacket. MDPE is chosen for its flexibility as well as excellent chemical resistance. However, MDPE lacks density and strength when compared to HDPE, making the two materials suitable for different applications.

Jacket Thickness Measurement

To characterize the jacket of Cable Type E, both experimental measurements and standard-based calculations were employed. According to IEC 60502-1, the nominal jacket thickness (ts) for low-voltage cables shall be calculated using the following formula:

$$t_s = 0{,}035 \cdot D + 1{,}0 \qquad (1)$$

where D is the fictitious diameter immediately under the jacket, in millimeters. Using a high-precision digital caliper, the measured value of D was measured as 27,1 mm. Substituting into the formula yields:

$$t_s = 0{,}035 \cdot 27{,}1 + 1{,}0 = 1{,}9485\ mm$$

According to the standard's rounding convention, the nominal jacket thickness is therefore taken as 2 mm. In addition to the theoretical value, the actual jacket thickness was determined experimentally by taking ten measurements around the circumference of each of two separate samples, using a digital caliper. The measurements are:

Table 13: Jacket thickness measurements (in mm) for two samples of cable Type D.

Jacket Thickness(mm)	1	2	3	4	5	6	7	8	9	10
Sample 1	**2,15**	**2,21**	**2,23**	**2,31**	**2,39**	**2,46**	**2,54**	**2,24**	**2,17**	**2,55**
Sample 2	**2,12**	**2,48**	**2,19**	**2,10**	**2,33**	**2,28**	**2,38**	**2,18**	**2,40**	**2,54**

Calculated average of sample 1: 2,325 mm → 2,3 mm

Calculated average of sample 2: 2,3 mm → 2,3 mm

Calculated Type D jacket thickness average: 2,3125 mm → 2,3 mm

A comparison between the theoretical and experimental results reveals that the measured jacket thickness of 2,3 mm exceeds the nominal value of 1,9 mm calculated according to the standard. This difference may stem from manufacturing variability, non-uniformity induced by the cable's screen, or small deviations from the measuring process. For the purposes of this study, the experimentally obtained jacket thickness will be used in subsequent analyses.

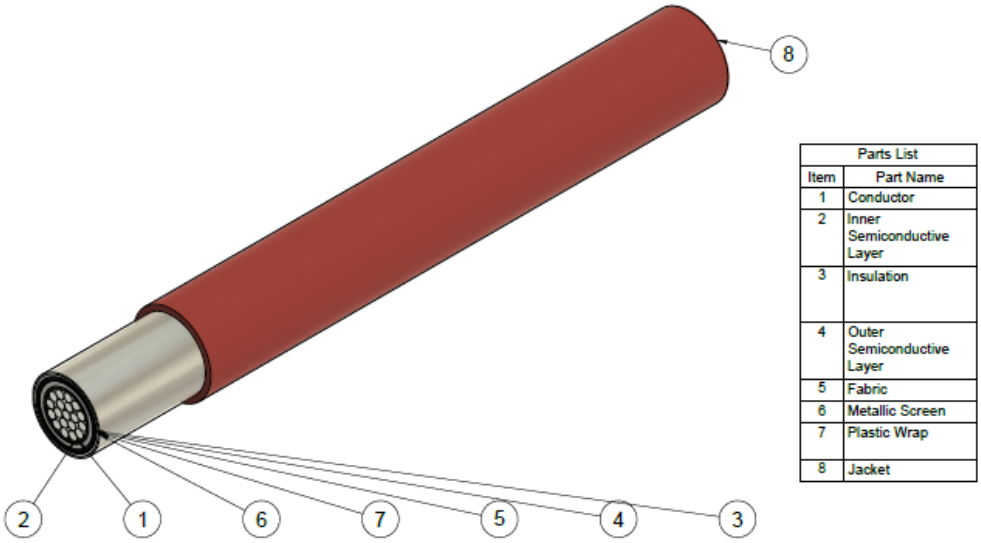

Parts List	
Item	Part Name
1	Conductor
2	Inner Semiconductive Layer
3	Insulation
4	Outer Semiconductive Layer
5	Fabric
6	Metallic Screen
7	Plastic Wrap
8	Jacket

Figure 11: 3D model of Cable Type D with numbered structural layers and parts list.

Figure 12: Photographs of the actual Cable D sample used in the experimental setup: (left) side view of the cable segment with partially stripped outer sheath, and (right) cross-sectional view showing the conductor bundle, insulation, and exposed screen layers.

3.2.5 Cable Type E: 1 kV, XLPE, SWA, PVC

Cable Type E is a low to medium voltage, three-core cable, rated for operation at 1 kV. It is manufactured in accordance with IEC 60502-1, which specifies in construction and performance for power cables with extruded insulation for rated voltages up to 3 kV. The cable's design complies with fixed installation requirements for power distribution and industrial applications, prioritizing safety and durability [3].

Construction and Materials

This cable is constructed with three stranded aluminum conductors, each with a cross-sectional area of 240 mm², making it suitable for high-load, low-voltage applications such as industrial power distribution. A thin inner semiconductive layer is extruded to smooth the electric field interface between the conductor and insulation. The insulation is made of XLPE, offering high dielectric strength and thermal resistance. The three individually insulated and screened cores are then laid together and wrapped in a PVC bedding layer, protecting the cores during armour application. Over the bedding, a layer of steel wire armour (SWA) is helically applied. The SWA enhances the cable's mechanical durability, enabling it to withstand physical damage and extreme conditions. Finally, the cable is covered with a black PVC outer sheath, providing environmental resistance and mechanical protection.

Jacket Thickness Measurement

To characterize the jacket of Cable Type E, both experimental measurements and standard-based calculations were employed. According to IEC 60502-1, the nominal jacket thickness (t_s) for low-voltage cables shall be calculated using:

$$t_s = 0{,}035 \cdot D + 1{,}0 \qquad (1)$$

Substituting into the formula yields:

$$t_s = 0{,}035 \cdot 51{,}2 + 1{,}0 = 2{,}792\ mm$$

Following the standard's rounding rule, the nominal sheath thickness is therefore taken as 2,8 mm.

In addition to the theoretical value, the actual outer jacket thickness was experimentally determined by taking ten circumferential measurements from each of two separate cable samples, using a digital caliper.

Table 14:Jacket thickness measurements (in mm) for two samples of cable Type E.

Jacket Thickness (mm)	1	2	3	4	5	6	7	8	9	10
Sample 1	**2,64**	**2,61**	**2,50**	**2,42**	**2,41**	**2,30**	**2,36**	**2,43**	**2,48**	**2,39**
Sample 2	**2,74**	**2,47**	**2,45**	**2,36**	**2,40**	**2,37**	**2,34**	**2,44**	**2,60**	**2,66**

Calculated average of sample 1: 2,454 mm → 2,5 mm

Calculated average of sample 2: 2,483 mm → 2,5 mm

Calculated Type E jacket thickness average: 2,4685 mm → 2,5 mm

Comparing the results, it is evident that the experimentally measured value (2,5 mm) is lower than the nominal theoretical value (2,8 mm). This deviation may be attributed to manufacturing tolerances or minor inaccuracies in manual measurement. The observed difference highlights the importance of combining theoretical standards with empirical verification. The experimentally measured jacket thickness will be considered for further analysis, as it more accurately reflects the actual physical characteristics of the cable.

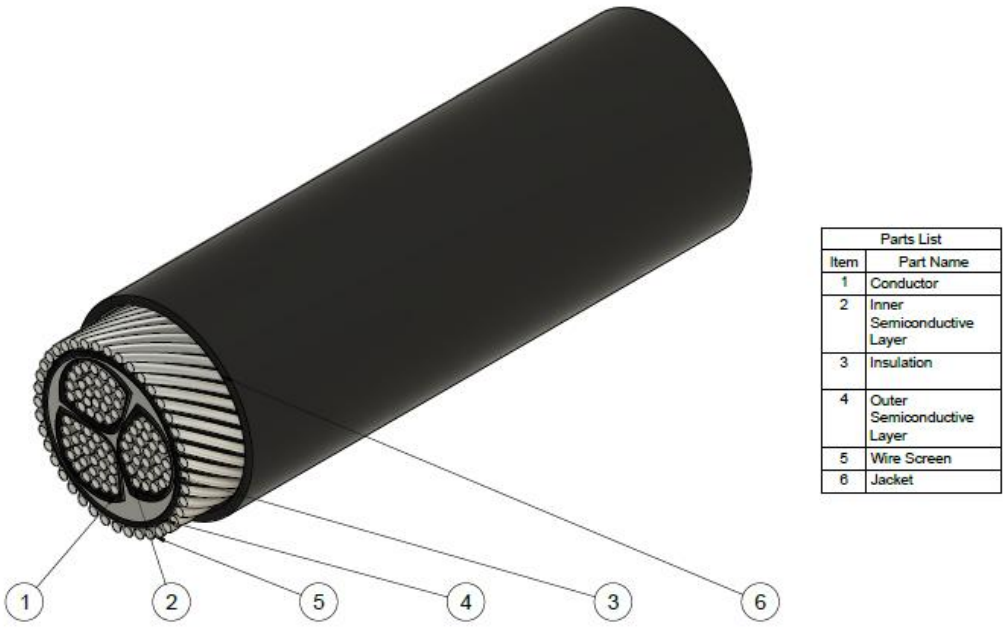

Figure 13:3D model of Cable Type E with numbered structural layers and parts list.

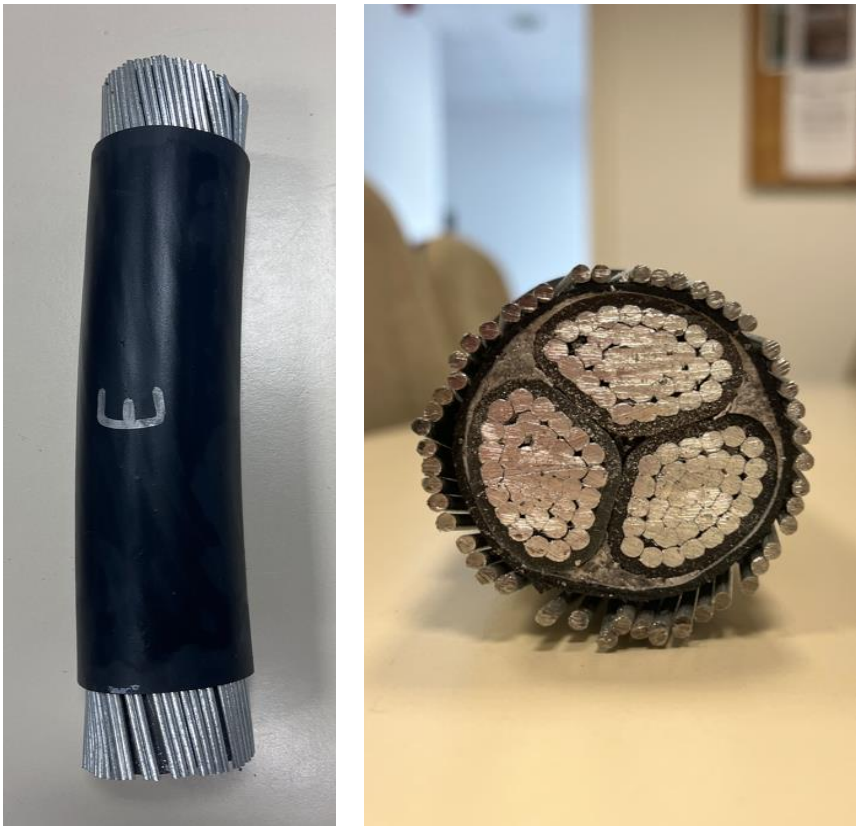

Figure 14:Photographs of the actual Cable E sample used in the experimental setup: (left) side view of the cable segment with partially stripped outer sheath, and (right) cross-sectional view showing the conductor bundle, insulation, and exposed screen layers.

3.3 Experimental Setup and Procedure

This chapter presents the experimental configuration developed to evaluate the dielectric strength of medium voltage cable jackets under impulse voltage conditions. It details the selection of the dielectric medium, the evolution of the test tank designs, and the comprehensive layout of the electrical test system, including the impulse voltage generator, voltage divider, and oscilloscope interface. The aim is to recreate realistic overvoltage scenarios in a controlled laboratory environment, simulating transient phenomena such as lightning surges.

3.3.1 Dielectric Medium and Test Tank

To ensure electrical insulation and suppress unwanted discharges during testing, the cable samples were fully immersed in a dielectric medium. Specifically, an EKO transformer-grade mineral insulated oil was selected, formulated with antioxidant additives to enhance its oxidation stability. The oil consisted primarily of hydrotreated light naphthenic distillates (petroleum), known for their stable dielectric performance.

The selected oil falls under the classification of Type A inhibited, conforming to IEC 60296 specifications. It contains an antioxidant concentration of 0,36% by weight, delivering higher oxidation stability. Most importantly, following proper filtration and degassing treatment, the oil demonstrated a breakdown voltage of 75 kV, measured with a 2,5 mm electrode gap. This confirms its effectiveness in withstanding high-voltage impulse stress conditions and its reliability as a test medium for dielectric strength evaluations [21].

Table 15: Electrical and Physical Characteristics of EKO Insulating Oil [22].

Properties	Units	Methods	EKO INSULATING OIL
Density at 20°C	g/ml	ISO 12185	0.875
Breakdown voltage, before treatment, 2,5 mm	kV	IEC 60156	57
Breakdown voltage, after treatment, 2,5 mm	kV	IEC 60165	75
Dielectric Dissipation Factor (DDF) at 90°C		IEC 60247	0,001

During the course of the experiment, three different test tanks were employed to house the dielectric medium and support the cable samples. The initial tank configuration was a rectangular

container with dimensions 40 × 40 × 20 cm, made of transparent plexiglass, designed to allow full visual access to the sample during testing. The panels were joined at the corners using an adhesive bonding method. During operation, the tank was filled with the dielectric oil and the cable sample was submerged. However, the cable was positioned close to one of the vertical corners of the tank, adjacent to a glued interface.

Under impulse voltage conditions, the sharp 90° plexiglass corner acted as a site of electric field intensification, particularly at the interface between the dielectric oil, the cable, and the tank wall. This localized enhancement of the electric field resulted in concentrated electrical and mechanical stresses. Sharp dielectric corners are known to cause irregular field behavior and abrupt variations in surface impedance, which can lead to stress accumulation along boundary interfaces. In this configuration, the combined stresses at the bonded corner exceeded the mechanical integrity of the adhesive, initiating partial discharges and leading to structural failure in the form of cracking and oil leakage. Consequently, the tank was deemed unsuitable for further testing [23].

Figure 15:Overview of the first dielectric oil tank (left) and experimental arrangement with cable sample (right).

The second test tank was constructed from plexiglass in a triangular prism shape with approximate dimensions of 40 × 35 × 25 cm. Like the first tank, it was filled with dielectric oil

and used for impulse voltage testing of immersed cable samples. Despite the modified geometry, failure occurred again near a glued corner where the electric field intensified. The concentrated stress at the junction led to partial discharges and cracking of the bonded seam.

Figure 16: Overview of the second experimental oil tank arrangement with cable sample.

The third and final experimental configuration utilizes two plastic containers, nested one inside the other, with overall external dimensions of 60 × 39 × 20 cm. This dual-container arrangement was implemented as a safety measure to prevent oil spills in the event of leakage or accidental tank failure during impulse voltage testing. In contrast to the previous transparent plexiglass constructions, the final setup used black plastic containers, which, although lacking the advantage of visual transparency, provided improved mechanical durability.

To prevent potential partial discharges or surface tracking between the cable and the container walls, a plastic holder with custom-made semicylindrical grooves was employed. This design securely supports the cable at a fixed height within the oil, maintaining uniform clearance from all surrounding surfaces. Also, the cable sample was centrally positioned within the tank, effectively eliminating the chances of breakage. This final design eliminated weak points observed in previous tank geometries and successfully withstood all voltage impulses without discharge activity or mechanical damage.

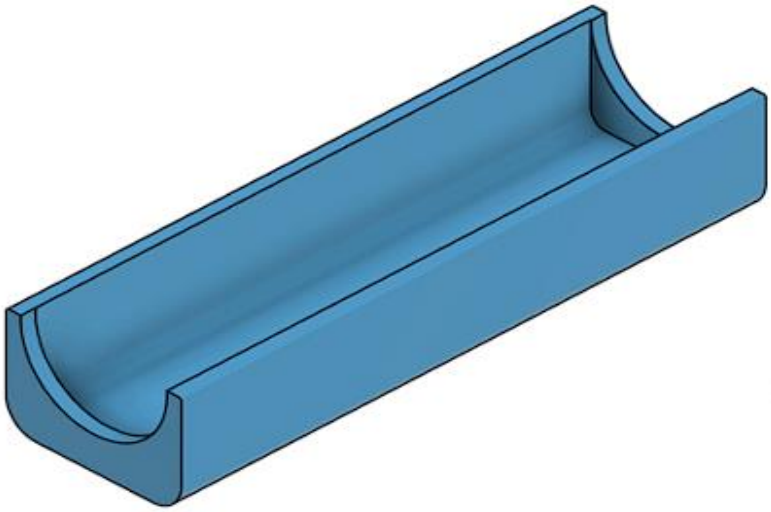

Figure 17: 3D model of the custom semicylindrical plastic holder.

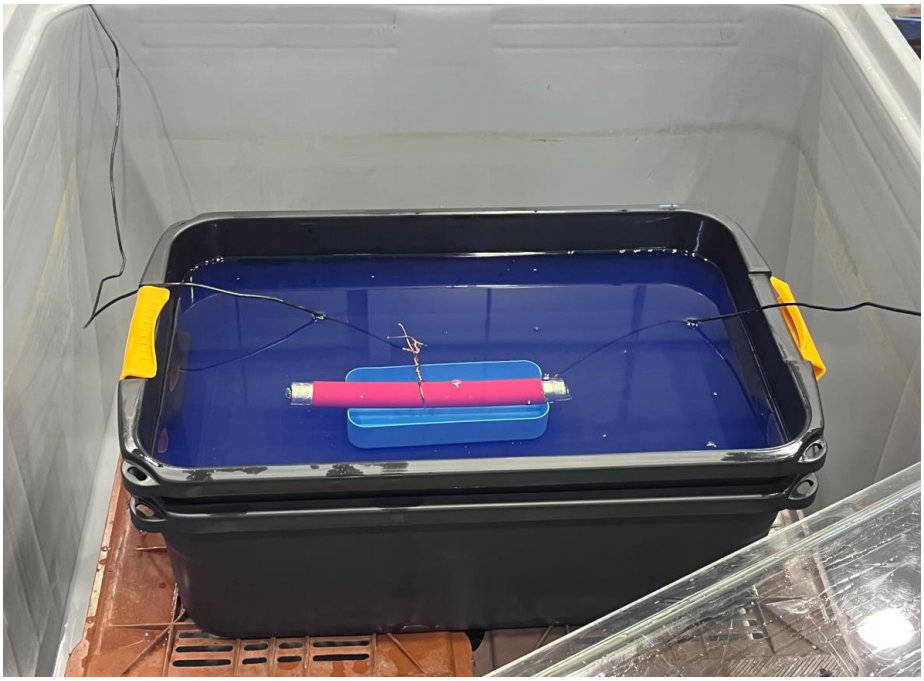

Figure 18: Overview of the final test setup using plastic containers with cable sample.

To ensure safe operating conditions and contain any accidental oil leakage, all test setups were placed inside a large, high-capacity plastic containment box with approximate dimensions of 1,00 × 1,40 × 0,70 m. This secondary enclosure served as a protective barrier against environmental contamination and minimized the risk of slipping hazards or equipment damage in the event of tank failure or dielectric fluid overflow.

Figure 19: Safety containment box that houses the test tanks.

3.3.2 Electrical Configuration

To successfully conduct the experiment, a high voltage test system was developed in order to apply controlled overvoltage waveforms representative of real-world electrical stress conditions.

- **Impulse Voltage Generator**

To simulate high voltage transients, an impulse voltage generator is utilized to generate overvoltage waveforms for evaluating the dielectric strength of medium voltage samples. Specifically, a five-stage Marx generator was used, capable of delivering 100 kV per stage, summing up to 500 kV. This type of generator is employed due to its ability to produce a smooth full lightning-impulse voltage having a front time of 1,2 μs and a time to half-value of 50 μs and described as a 1,2/50 μs impulse [13].

Figure 20:Front view of the five-stage Marx generator.

The Marx generator operates on the principle of charging capacitors in parallel and discharging them in series to multiply voltage. In its charging phase, all capacitors are slowly energized to the same DC voltage level via high-resistance resistors. Once charged, a triggering mechanism initiates a breakdown across the spark gaps, rapidly connecting the capacitors in series. This conversion multiplies the voltage by the number of stages, producing a high-voltage impulse that mimics real-world transients [24].

The initial breakdown is typically triggered by a controlled discharge in the first gap, causing a cascading effect, where subsequent gaps fire in rapid succession. This creates a series-connected pathway through which the stored energy is released almost instantaneously. The waveform exhibits a sharp voltage rise followed by an exponential decay, replicating the required 1,2/50 μs waveform.

The impulse voltage generator consists of several independent components, each contributing to the generation of standardized high voltage waveforms used for dielectric testing. First and foremost, the charging source for the Marx generator is a direct current generator. It converts the standard 220 V AC supply into a controllable high voltage DC output of up to 100 kV, with a maximum charging current of 0,03 A. This unit is responsible for energizing the capacitors of the Marx generator.

Figure 21: Nameplate of the Direct Current Generator.

The energy required for impulse generation is stored in five capacitors, each rated at 100 kV, with a capacitance of 0,5 μF. When fully charged, the energy that they collectively store is Q = 12,5 kJ, calculated using the expression $Q = \frac{1}{2} C_c V_{charge}^2$. This energy is subsequently released in a controlled series discharge to create the test waveform.

Figure 22: Nameplate of the Marx generator capacitor.

Each storage capacitor is charged through a 3500 Ω charging resistor. These resistors serve to limit the charging current, allowing the capacitors to reach the target voltage gradually without undergoing thermal or electrical overstress. Once the discharge phase begins, these resistors are electrically out of the circuit and do not influence the impulse waveform.

Figure 23: Charging resistors and their highlighted position in the generator (left) and rating label (right).

Impulse generation begins with a controlled triggering mechanism consisting of a Trigatron spark gap and a dedicated trigger capacitor. The Trigatron consists of a high-voltage spherical electrode, a grounded spherical main electrode, and a trigger electrode mounted concentrically

through an insulated bushing. When all five capacitors are fully charged, the trigger capacitor, in this case rated at 250 pF and 100 kV, discharges into the trigger electrode. This creates an initial spark between the trigger and grounded spheres. The resulting space charge and electric field distortion induce a full breakdown across the main gap. This first breakdown initiates a cascade through the remaining spark gaps, rapidly reconfiguring the generator from a parallel to a series circuit. Compared to traditional three-electrode gaps, the Trigatron offers more precise control and requires a lower trigger voltage, making it a reliable choice for modern high-voltage impulse systems [25].

Figure 24: Trigger capacitor installed at the Marx generator.

To control the rise time of the impulse waveform, the generator includes five front resistors, each with a value of 12 Ω and installed in the output path. These resistors limit the peak current during the initial part of the discharge, shaping the waveform's front edge and reducing oscillations. Their combined effect contributes to achieving the standardized 1,2 μs rise time, which is critical for impulse testing.

Figure 25: Front resistors and their highlighted position in the generator (left) and rating label (right).

The generator uses five tail resistors, each rated at 150 Ω, to define the decay portion of the impulse waveform. These resistors form the discharge path after the waveform peak and are primarily responsible for establishing the 50 μs tail time. Additionally, they help dampen residual oscillations and dissipate energy, allowing the generator to recover quickly between impulses.

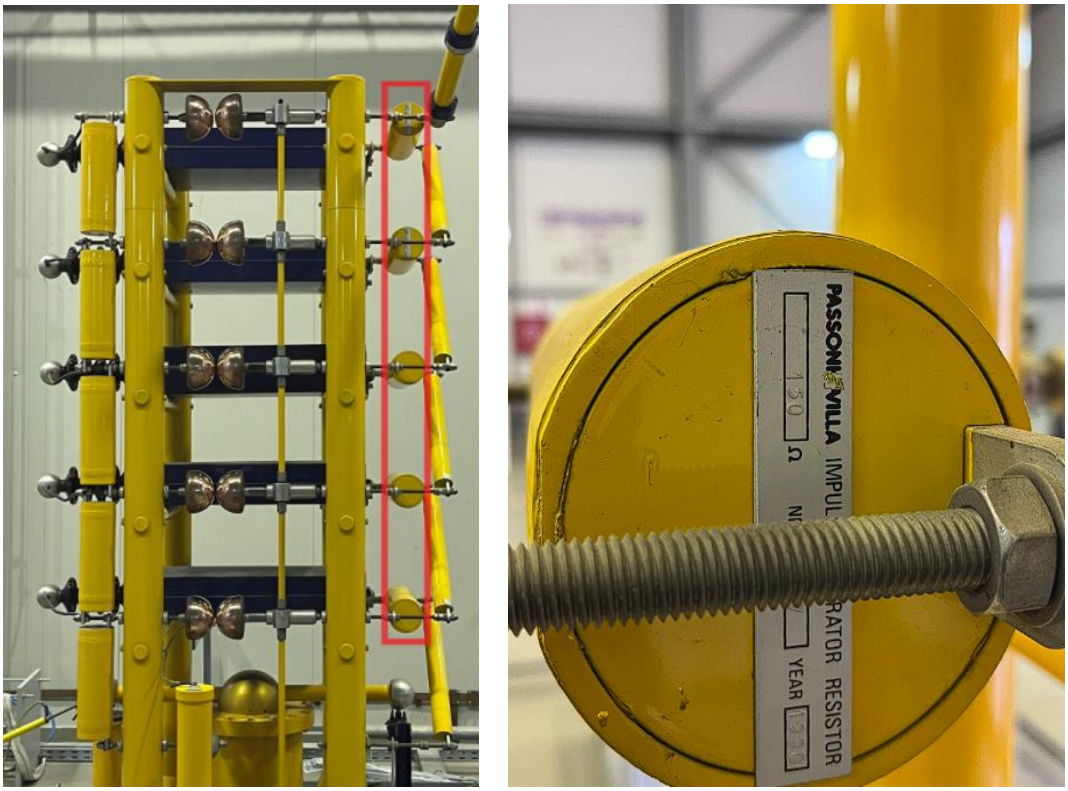

Figure 26: Tail resistors and their highlighted position in the generator (left) and rating label (right).

At the final stage of the impulse path, three output resistors are used to fine-tune the impedance between the generator and the test object. Two of these resistors are rated at 25 kV, and one is rated at 35 kV. Their function is to stabilize the impulse waveform as it exits the generator, preventing reflections and distortion that could affect the accuracy of the test or damage the measuring equipment.

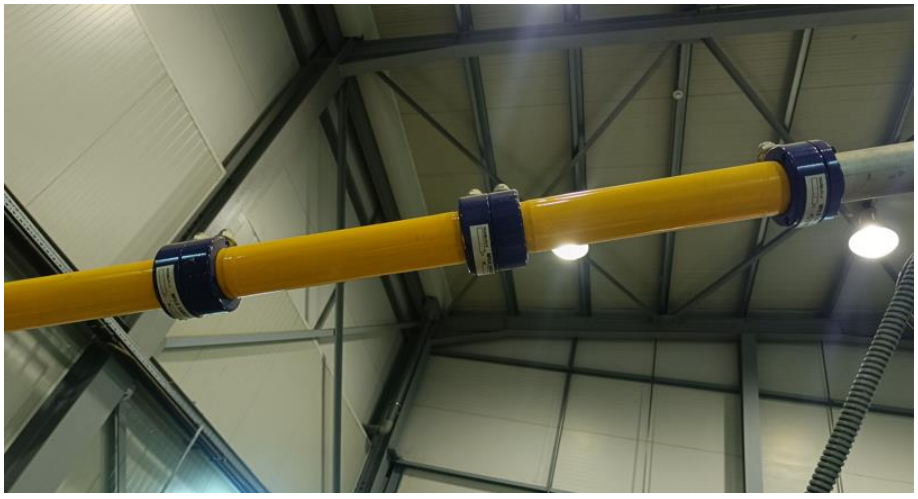

Figure 27: Output resistors of the Marx generator.

Spark gaps form the essential switching elements of the Marx generator. They maintain electrical isolation during the charging phase and enable synchronous switching during discharge. The spark gaps are designed to break down slightly above the charging voltage threshold, and their coordinated breakdown initiates the formation of the impulse voltage. In order to prevent carbon deposits and ensure consistent breakdown behavior, the spark gaps were cleaned using sandpaper and anti-corrosion paste, confirming their effective operation.

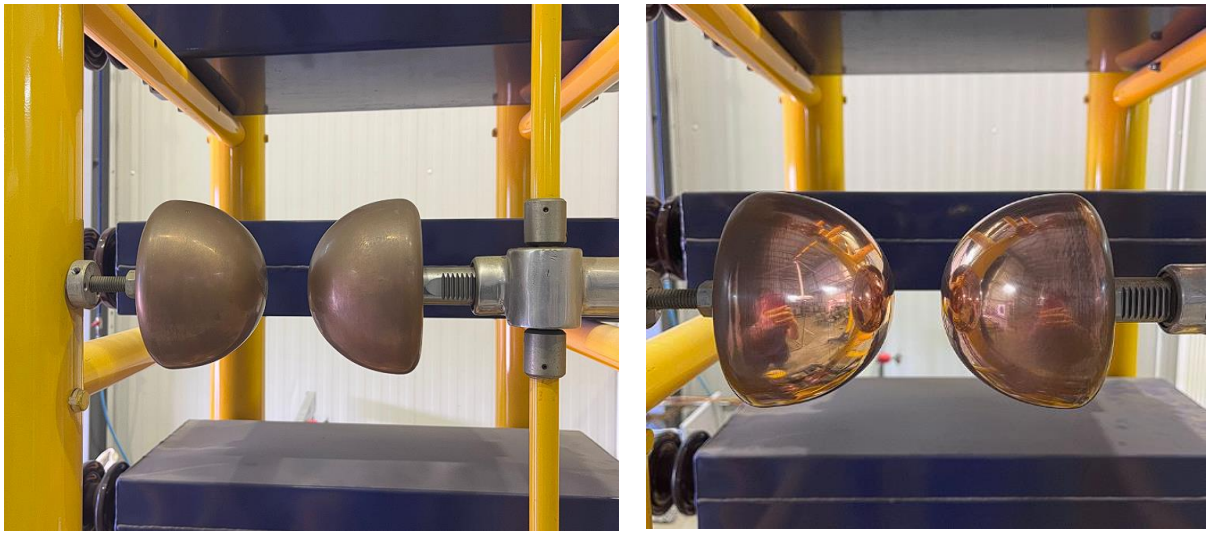

Figure 28: Spark Gap electrodes before (left) and after polishing(right).

While the five-stage Marx generator was originally designed to produce impulse voltages up to 500 kV in its standard configuration, such performance exceeded the voltage levels typically associated with medium-voltage jacket testing. Therefore, in order to target the appropriate voltage spectrum and deliver impulses closer to 100 kV, the generator was reconfigured into a parallel arrangement. This shift allowed the system to operate effectively within the dielectric strength range expected of medium-voltage cable systems.

In its high-voltage mode, the generator adopts a 4-series × 1-parallel configuration, in which four stages are connected in series while a single path remains parallel. This setup enables the output voltage to scale proportionally with the number of stages, theoretically reaching up to 500 kV, as each capacitor contributes its full voltage to the total output. However, this also reduces the equivalent capacitance of the system, resulting in lower output current during discharge.

For medium-voltage testing, the generator was instead configured in a 1-series × 5-parallel arrangement, connecting all five stages in parallel. This does not increase the output voltage

beyond the rating of a single stage (100 kV), but it multiplies the total capacitance, as the capacitance values of the stages add up directly. While the total energy stored in both configurations remains equal and the product of total capacitance and voltage squared is preserved, the way that energy is delivered differs. The parallel setup enables the delivery of higher current pulses, which is particularly valuable for testing the energy absorption and insulation breakdown behavior of medium-voltage cables.

This reconfiguration process is illustrated in Figure 32, where both the high and medium voltage topologies are depicted side by side. Each configuration involves the same core component charging resistors (R_c), capacitors (C), front resistors (R_f), and tail resistors (R_t), however their interconnections are altered to match the desired test parameters.

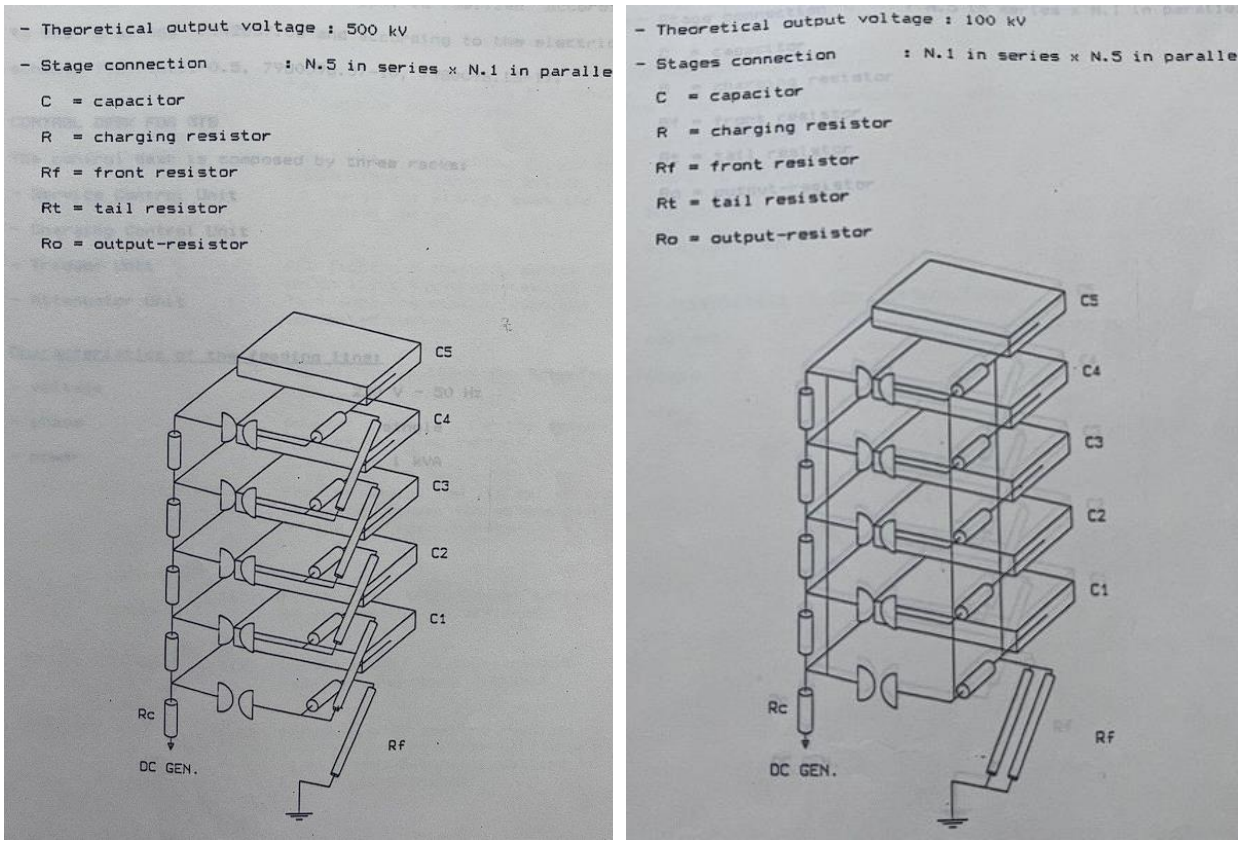

Figure 29: 500 kV and 100kV configurations from the manufacturer's manual. 4×1 series mode for 500 kV generation (left), 1×5 parallel arrangement for 100 kV output (right).

The reconfiguration process involved the conversion of the Marx generator from a series to a parallel configuration. In its original setup, the five capacitors were stacked in series to produce high output voltages. To adapt the system for medium-voltage testing, these capacitors were rewired to operate in parallel, thereby maintaining a lower output voltage while increasing the available discharge current. This required a complete redesign of the internal wiring harness and the integration of custom copper bus bars to ensure uniform voltage distribution and secure mechanical support.

Figure 30: Copper bus bar used for parallelizing capacitors.

In the modified parallel configuration, each capacitor remained paired with its own 3500 Ω charging resistor (R_c). Instead of being interconnected as in the series arrangement, each resistor was now linked directly to the output of the DC charging unit through individual conductors. This approach allowed each capacitor to charge independently, ensuring a uniform voltage distribution and eliminating the risk of unequal charging currents between units.

Figure 31: Short insulated conductor used for connecting charging resistors (R_c) to the DC source.

Additionally, the discharge circuit needed to be reconfigured. Originally, each stage of the Marx generator had its own tail resistor. In the new parallel setup, these resistors were removed from their individual positions and instead connected together as a single group after the capacitor bank. This change lowered the total tail resistance, which was necessary because connecting the capacitors in parallel increased the overall capacitance. By reducing resistance, the impulse tail time could still meet the standard requirement of around 50 μs.

Similarly, front resistors were recalculated to adapt to the altered front time caused by the parallel configuration. With the larger capacitance accelerating the rise time, the front resistors were reduced in value to preserve the standard 1,2 μs front time. Triggering accuracy was another critical factor. The spark gaps, including the Trigatron-triggered stage, were also evaluated and realigned to ensure simultaneous triggering across all parallel branches. This was essential to guarantee uniform breakdown behavior and stable waveform generation.

Figure 32: Left and right view of the Marx generator parallelized configuration.

- **Voltage Divider**

A capacitive voltage divider was employed to accurately scale down the high-voltage impulse waveform to measurable levels suitable for signal acquisition. The device supports impulse voltage measurements up to 500 kV (1,2/50 μs) and 360 kV (250/2500 μs). It incorporates a loading capacitor with a rated capacitance of 4000 pF, ensuring high precision and stability during transient measurements.

The divider is constructed with one high-voltage unit, meaning its internal components are calibrated to produce a reliable low-voltage replica of the high-voltage impulse signal. This scaled-down signal is then transmitted to the digital oscilloscope for waveform recording. By using this voltage divider, the system complies with IEC 60060-1 guidelines for accurate and safe high-voltage measurements, enabling detailed analysis of peak voltage, waveform shape, and temporal parameters such as front and tail time [13].

Figure 33: Impulse Voltage Divider (left) and its technical specifications (right).

- **Digital Oscilloscope and Control Interface**

Waveform acquisition and analysis were performed using a Teledyne LeCroy WaveRunner 604Zi digital oscilloscope. This instrument was connected to the output of the capacitive voltage divider to record the impulse voltage waveforms generated during testing. It offers high sampling rates and bandwidth, making it suitable for capturing fast transient events such as 1,2/50 μs lightning impulses. Its advanced triggering and measurement capabilities allowed for precise determination of peak voltage, front time, and tail time.

The Marx generator is operated through a dedicated control interface that allows precise management of charging, triggering, and discharging processes. This interface includes essential functions such as voltage setting, charge monitoring, timing control, and emergency shutdown. The system provides real-time feedback on generator status and enables controlled triggering of the impulse event, ensuring synchronization with measurement equipment and adherence to safety protocols during high-voltage testing.

Figure 34: Digital oscilloscope and Marx generator control interface.

3.4 Mathematical Analysis and Simulation of the Impulse Voltage Generator

3.4.1 Computation of the Time and Energy Constants

Front time constant T_f

The front time constant T_f determines the voltage rise portion of the impulse waveform and is primarily influenced by the resistive-capacitive shaping network. An approximate expression for T_f is:

$$T_f = 3 \cdot R_2 \cdot C_2 \cdot \frac{C_1}{C_1 + C_2} \quad (2)$$

Substituting the known values into the equation:

$$Tf = 3 \cdot 91\Omega \cdot 4 \cdot 10^{-9}F \cdot \frac{2{,}5 \cdot 10^{-6}F}{2{,}5 \cdot 10^{-6}F + 4 \cdot 10^{-9}F} \approx 3 \cdot 91 \cdot 4 \cdot 10 - 9 \cdot 0{,}998 = 1{,}09\mu s$$

This result satisfies the IEC 60060-1 standard for front time having ±30% tolerance, that means that acceptable values are in range 0,84 μs to 1,56 μs [13].

Tail time constant T_t

The tail time constant T_t, which characterizes the decay of the waveform after the peak, is primarily determined by the discharge resistor R_1 and the combined capacitance:

$$T_t = 0{,}693 \cdot (C_1 + C_2) \cdot R_1 \quad (3)$$

Substituting the known values into the equation:

$$T_t = 0{,}693 \cdot (2{,}5 \cdot 10^{-6}F + 4 \cdot 10^{-9}F) \cdot 30 = 52{,}06\,\mu s$$

This result closely matches the nominal tail time of 50 μs, falling within the allowable ±20% range defined by IEC 60060-1 (40 μs to 60 μs) [13].

Charging time: The large charging resistor $R_c = 3500$ and capacitor bank $C_1 = 2{,}5\mu F$ form the charging time constant:

$$\tau_{\text{charge}} = R_c \cdot C_1 = 3500 \cdot 2{,}5 \times 10^{-6} = 8{,}75\ \text{ms}$$

This value ensures relatively fast recharging between impulse applications.

Peak voltage and current: Although the parallel configuration keeps the output voltage limited to 100 kV (equal to a single stage), it significantly increases the available discharge current due to the increased capacitance.

Energy stored: Total stored energy in capacitor bank is:

$$E = \frac{1}{2} C_1 V^2 = \frac{1}{2} \cdot 2{,}5 \cdot 10^{-6} \cdot (100 \cdot 10^3)^2 = 12.5 \text{ Joules}$$

3.4.2 Simulation of Parallel Impulse Voltage Generator using ATP

To verify the expected impulse behavior and validate theoretical design assumptions, a full transient simulation of the parallel Marx generator configuration was performed using ATP-EMTP software. The goal was to simulate the dynamic discharge process and analyze the resulting impulse waveform under realistic electrical conditions.

The equivalent circuit replicated the actual hardware setup and included:

- **Charging Resistor:** $R_c = 3500\ \Omega$
- **Capacitor Bank**: $C_1 = 2.5\ \mu F$
- **Shaping Capacitor:** $C_2 = 0{,}004$ nF
- **Tail and Front Resistors:** $R_1 = 36\ \Omega$, $R_2 = 85\ \Omega$

The modeled equivalent circuit constructed from these elements is pictured below:

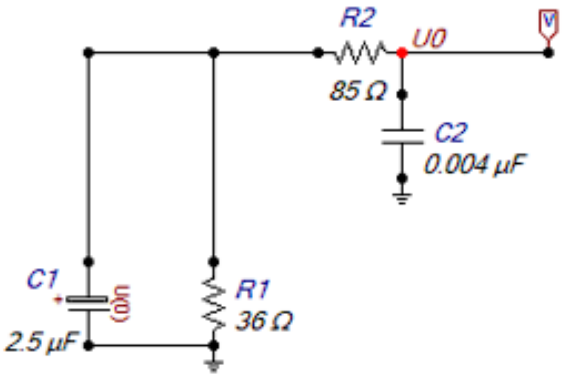

Figure 35: Equivalent Circuit of the Parallel Marx Generator Simulated in ATP-EMTP.

After constructing the model and initiating the triggering event, the output voltage waveform was recorded at the generator's output terminal. This waveform was then post-processed in MATLAB to extract key impulse characteristics. The measured front time T_1 was 1,028 μs, and the tail time T_2 was 54,915 μs, both of which fall within the allowable tolerances specified for a standard 1.2/50 μs lightning impulse waveform. The waveform fidelity index, calculated as η=0,978, indicates a remarkably close match between the simulated and ideal double-exponential waveform.

Table 16: Simulation Results of the Output Voltage Impulse Waveform – Front Time, Tail Time, and Waveform Fidelity Index.

Timing Characteristics	
t_{30}	0,162 μs
t_{90}	0,778 μs
Front time T_1	1,028 μs
Tail time T_2	54,915 μs
Shape η	0,978

The output waveform exhibits the characteristic shape of a standard lightning impulse, featuring a rapid voltage rise to a peak value near –100 kV, followed by a gradual decay governed by the tail-shaping resistors. This confirms the successful generation of a 1,2/50 μs waveform, consistent with IEC 60060-1 specifications.

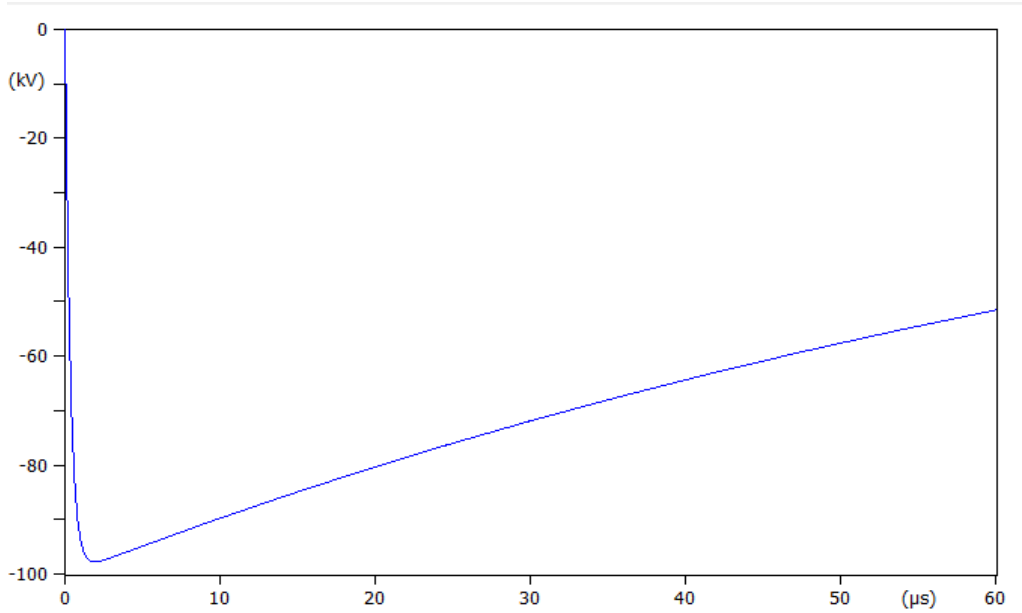

Figure 36: Output Signal of the Parallel Marx Generator Simulated in ATP-EMTP.

3.4.3 Theoretical and Simulated Comparison

The accuracy of the simulation was evaluated by comparing the front time (T_1) and tail time (T_2) against their corresponding theoretical values. The percentage deviation between the simulated and calculated results is presented in Table 17, providing a clear indication of the model's precision.

Table 17:Comparison of Theoretical and Simulated Waveform Times.

Parameter	Theoretical Value (μs)	Simulated Value(μs)	Deviation (%)
Front Time T_1	1,09	1,028	-5,69
Tail Time T_2	52,06	54,915	+ 5,49

The front time (T_1) shows a deviation of approximately −5.69%, which lies well within the ±30% tolerance defined by IEC 60060-1 for standard lightning impulses. Similarly, the tail time (T_2) deviates by +5.49%, remaining comfortably within the standard's ±20% limit. These results confirm the accurate selection of shaping resistors and capacitors, as well as the validity of the underlying analytical model. Additionally, the calculated waveform fidelity index ($\eta = 0.978$) reflects a high degree of conformity between the simulated output and the ideal double-exponential 1.2/50 μs lightning impulse, reinforcing the generator's performance and the credibility of the simulation process [13].

3.5 Overall Setup and Experimental Process

The experimental setup is organized into two main levels. The internal layout involves the preparation of the test sample and its submersion within the dielectric medium to ensure electrical isolation. In contrast, the external arrangement encompasses the impulse voltage generator, measurement instrumentation, and safety enclosures required for the controlled execution of high-voltage tests.

3.5.1 External Test Setup

The external test setup comprises the impulse voltage generator, measuring instrumentation, and the associated control and protection equipment arranged around the dielectric tank. The Marx generator, modified for medium voltage applications, is positioned adjacent to the test tank and serves as the voltage source for the dielectric strength tests. Its output is connected to the test

sample via shielded high voltage cables, while the ground reference is routed through a dedicated copper conductor.

A capacitive voltage divider is installed in series with the output to provide a scaled-down replica of the impulse waveform. This signal is fed into a digital oscilloscope, enabling real-time waveform capture and analysis. Both the divider and oscilloscope are configured according to IEC 60060-1 requirements for accurate peak voltage and waveform parameter assessment. To ensure operators' safety and maintain electromagnetic compatibility, the entire setup is isolated. Proper spacing between components, reinforced insulation distances, and mechanical support structures help accommodate the transient high currents associated with impulse discharge events.

Figure 37: External High-Voltage Setup.

3.5.2 Internal Tank Layout

For each sample subjected to testing, a conductive copper ring is securely positioned around the midpoint of the cable. This ring is connected through a dedicated grounding wire to the earth

terminal of the external impulse generator circuit, thereby establishing a well-defined reference potential throughout the test.

The opposite end of the cable sample is prepared by partially stripping the outer sheath, exposing the conductive layer beneath. This exposed section is connected to the high-voltage output terminal of the Marx generator through an appropriate impulse-rated clamp or connector. This arrangement ensures that the full test impulse is applied across the outer jacket of the cable. After establishing electrical connections, the entire sample is submerged in a dielectric oil-filled tank. The immersion medium prevents surface discharges and ensures uniform electric field distribution around the test object. This configuration enables controlled impulse application across the cable jacket, supporting reliable dielectric strength evaluation under standardized test conditions.

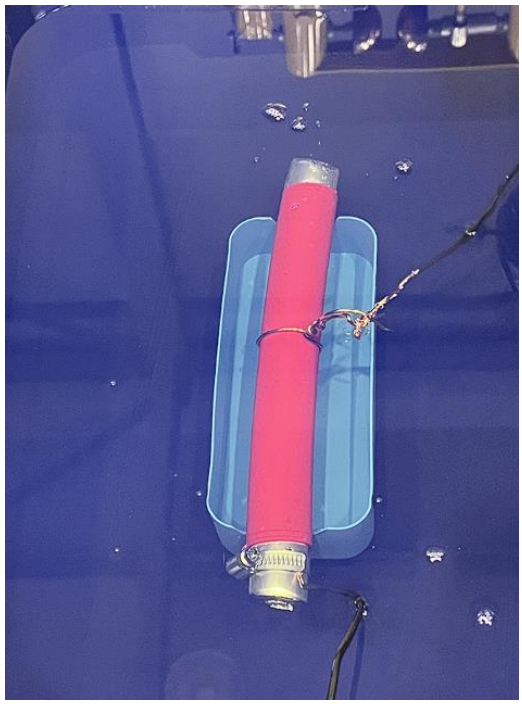

Figure 38: Internal Tank Layout.

3.5.3 Experimental Procedure

The main objective of this experimental process is to assess the dielectric strength of the cable jacket in medium voltage power cables. This is achieved by subjecting each sample to high-voltage impulses that simulate real-world transient conditions such as lightning events. The goal is to

determine how far the outer sheath can withstand voltage stresses beyond the rated level before jacket breakdown occurs.

Before testing, each sample is carefully cleaned using isopropyl alcohol to remove dust, moisture, or surface impurities that could interfere with the electrical performance or introduce testing anomalies. Each test follows a stepwise procedure. After preparing and connecting the cable inside the oil-filled tank, impulse voltages are applied in increasing steps of 5 kV. Starting near or slightly below the rated voltage, each level is applied seven times to the sample before progressing to the next level. The breakdown voltage is defined as the point at which the jacket cracks or fails to withstand the impulse without partial discharge. If no breakdown occurs, the sample continues to the next voltage level until failure is observed.

After the failure point is reached, visual inspection is performed to assess signs of jacket damage, such as burn marks, cracking, or dielectric puncture. These observations are documented in detail to classify the failure mode and correlate it with the electrical data. To ensure accuracy and traceability, each impulse application is recorded through a digital oscilloscope connected via a capacitive voltage divider. This system captures the full waveform and allows for verification against the standardized 1,2/50 μs shape defined by IEC 60060-1. Only impulses meeting waveform criteria for front time and tail time are considered valid for analysis, ensuring comparability across tests.

Each voltage application generates a screenshot of the waveform and a CSV data file, both of which are archived for post-test evaluation. These files support later analysis of voltage rise rates, overshoot, and energy dissipation trends. Applying each voltage level seven times improves the statistical reliability of the results and increases the chances of identifying marginal insulation defects that may not fail on a single application. This repetition also accounts for minor variations in test conditions and provides a more robust measure of the true dielectric endurance of the jacket material. The outcomes contribute to a broader understanding of cable reliability, offering insights into material performance, aging tolerance, and potential weaknesses that may not be evident through conventional testing alone.

3.6 Experimental Results and Breakdown Analysis per Cable Type

Each subsection documents the physical observations, breakdown voltages, and oscilloscope data corresponding to individual samples. Visual evidence of dielectric failure is supported by waveform analysis and tabulated voltage values. The tested cables vary in construction, voltage rating, and jacket material, allowing for comparative assessment of insulation performance under high-voltage stress.

3.6.1 Cable Type A: NA2XSY 20kV, CWS, PVC

The testing procedure began with Cable Type A, a NA2XSY 20 kV-rated medium-voltage cable featuring a copper wire screen (CWS) and a PVC outer jacket. Five individual samples were prepared, immersed in the oil-filled test tank, and subjected to standardized impulse voltage tests.

Each sample was securely mounted in the tank with copper wire loops used to establish high-voltage and ground connections. Figure 39 shows two of the Cable A samples immediately after experiencing dielectric breakdown. The black discoloration near the connection point is evidence of smoke or carbonization resulting from the high-energy discharge. This visual damage confirms the location of electrical failure and aligns with oscilloscope recordings of sudden voltage collapse.

Figure 39: Cable A samples immediately after an electrical breakdown.

During post-test handling, the samples were inspected for visible surface damage, carbonization, or puncture. These inspections were critical for correlating the breakdown waveform to the physical failure site. In most cases, the breakdown initiated near the copper loop, propagating outward through the jacket.

Figure 40: Visible breakdown markings and localized discharge path.

Impulse voltage traces were recorded during each test, with waveform oscillographs stored in the digital oscilloscope's memory. Two representative waveforms are shown below, corresponding to Sample 1 and Sample 2. Breakdown events are characterized by a sudden drop in voltage magnitude, with little or no recovery, indicating dielectric puncture.

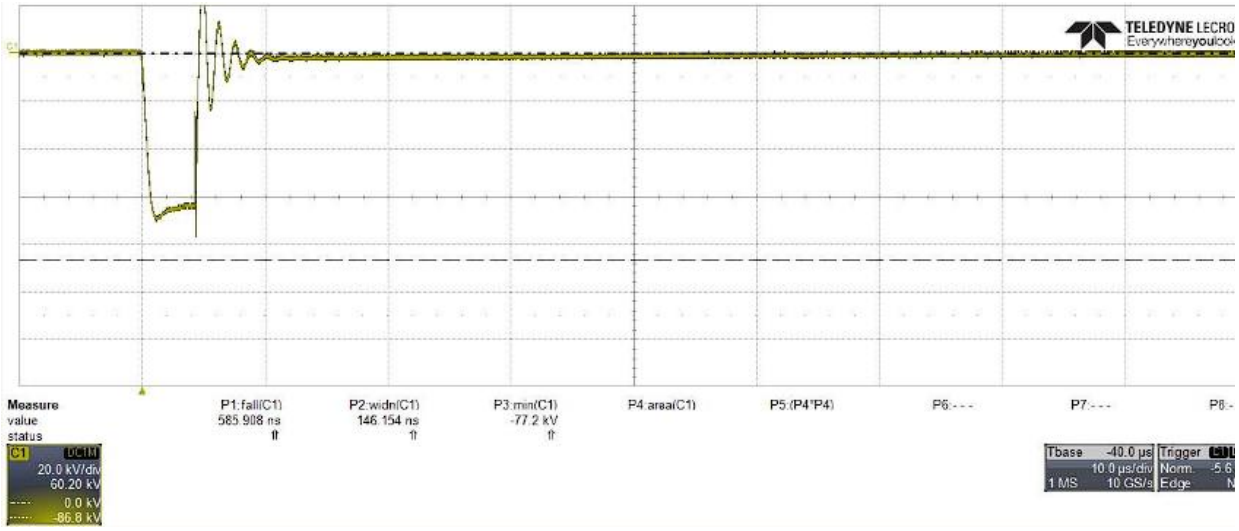

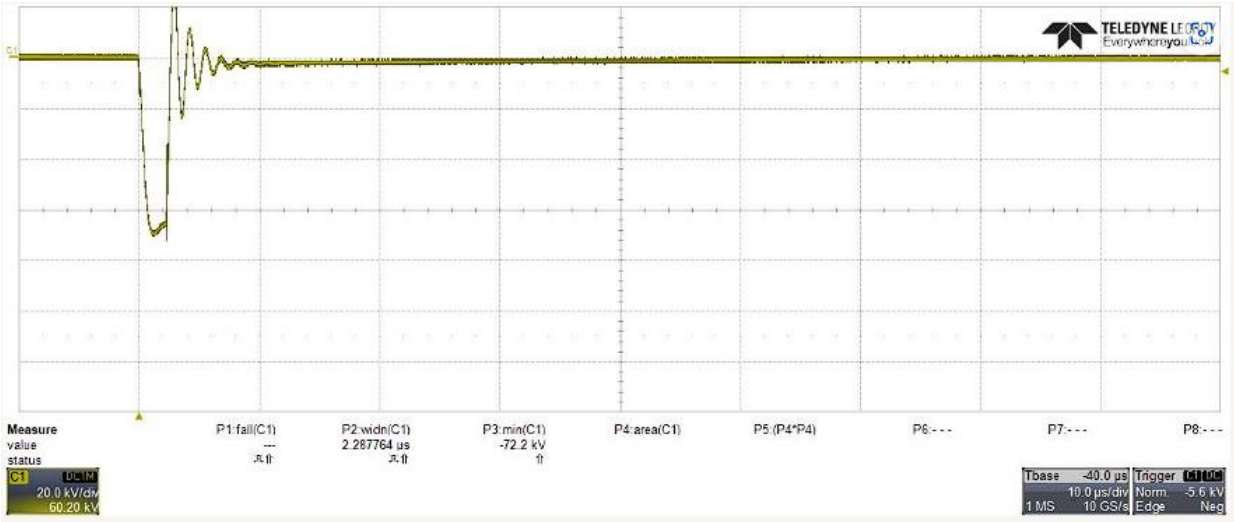

Figure 41: Oscillograph of impulse breakdown event for Sample 2 of Cable A (up) and oscillograph of impulse breakdown event for Sample 3 of Cable A (down).

In addition to the complete breakdown events recorded during testing, one sample showed a visible surface discharge along the outer PVC jacket. This was clearly observed during the post-test inspection and may have been partially captured by the oscilloscope, although it did not show the typical characteristics of a full dielectric puncture. The discharge likely occurred due to surface contamination or field intensification near the ground ring. Since it did not cause a puncture or interrupt the voltage waveform, it was not included in the breakdown voltage dataset. However, it is noteworthy as a non-destructive surface discharge and may indicate conditions that promote surface tracking on the jacket.

Figure 42: Surface discharge trace on the PVC jacket of Cable A.

All five samples of Cable Type A experienced breakdown within a relatively narrow range of impulse voltages, as summarized in Table 18. The minimum recorded breakdown voltage was −66.7 kV, while the maximum was −61.9 kV. The values are tightly clustered between −62 kV and −66.7 kV, indicating consistent dielectric behavior across the set. No samples exhibited significant early failure, suggesting an absence of severe manufacturing defects or surface anomalies in this batch.

Table 18: Breakdown voltage per sample for Cable Type A.

Breakdown Voltage per Sample	**Voltage (kV)**
Sample 1	-66,7
Sample 2	-66,2
Sample 3	-62,9
Sample 4	-65,2
Sample 5	-61,9

3.6.2 Cable Type B: 20kV, CWS, PPS+HDPE

Cable Type B consisted of a 20 kV-rated medium-voltage cable with a copper wire screen (CWS) and a dual-layer outer jacket made from a polypropylene-based semiconductive compound (PPS) overlaid with high-density polyethylene (HDPE). Following the same process, the cables were immersed in the oil-filled test tank and subjected to standardized impulse voltage tests.

Post-test visual inspection confirmed dielectric failure in all ten samples. In most cases, the breakdown site was identifiable by small punctures or burn marks on the jacket surface. One such failure is highlighted below.

Figure 43: Visible breakdown jacket marking in Cable B.

Representative impulse waveforms are shown below. These illustrate the characteristic behavior of Cable B during breakdown: a rapid voltage rise followed by a sharp collapse, with minimal overshoot or recovery, confirming electrical puncture.

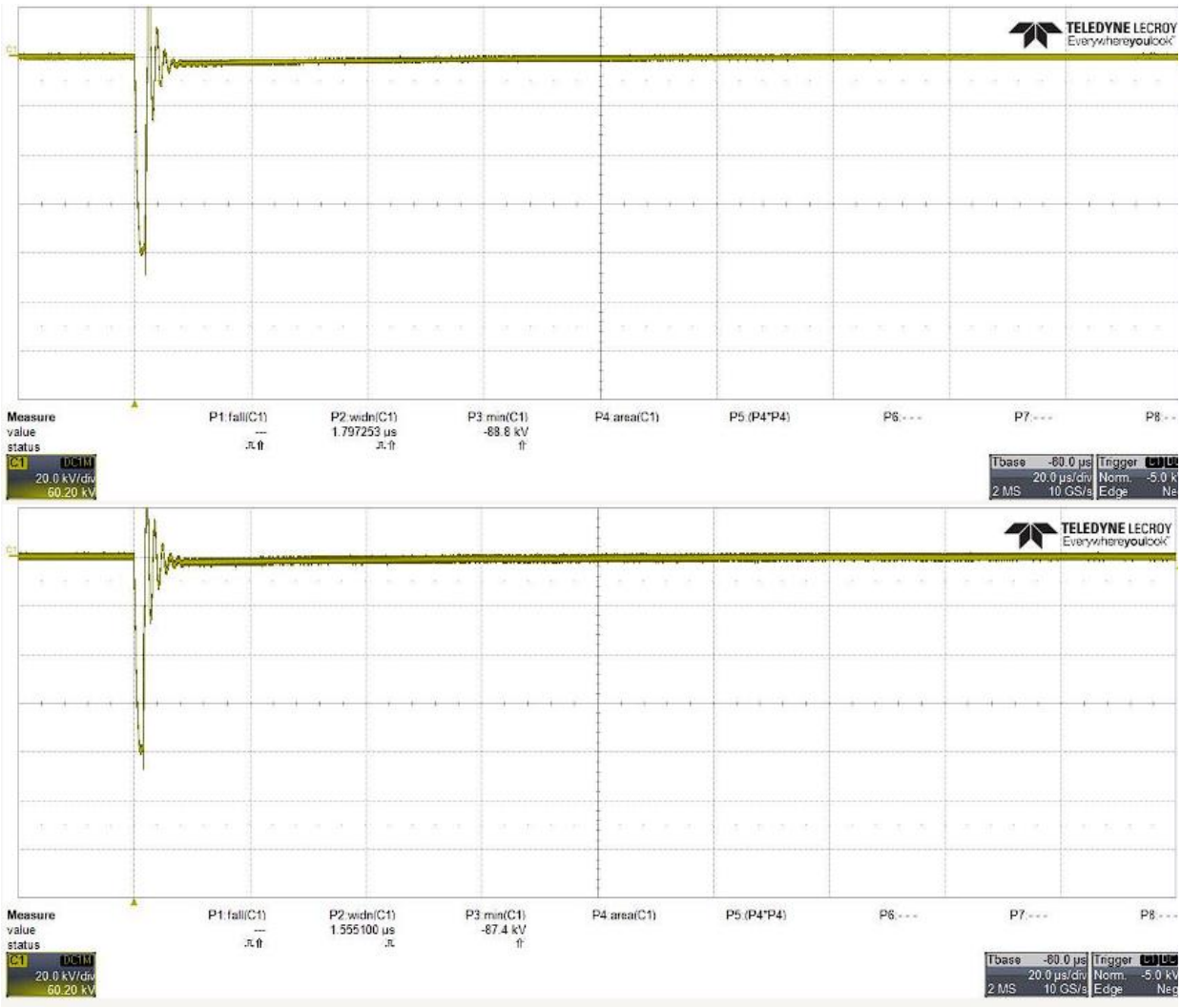

Figure 44: Oscillograph of impulse breakdown event for Sample 2 of Cable B(up) and oscillograph of impulse breakdown event for Sample 5 of Cable B(down).

The complete breakdown voltage dataset for Cable Type B is summarized in Table 19. The results show a tight clustering of breakdown voltages in the −71 kV to −78 kV range, with the exception of Sample 7, which failed at a slightly lower level of −69.4 kV. This suggests consistent dielectric performance across the batch, with minimal outliers.

Table 19: Breakdown voltage per sample for Cable Type B.

Breakdown Voltage per Sample	**Voltage (kV)**
Sample 1	-74,8
Sample 2	-71,6
Sample 3	-73
Sample 4	-74,2
Sample 5	-78,4
Sample 6	-77
Sample 7	-69,4
Sample 8	-77
Sample 9	-74,8
Sample 10	-71,6

3.6.3 Cable Type C: 20kV, AL-PE, HDPE

Cable Type C featured a 20 kV aluminum-conductor cable with a polyethylene insulated core and a high-density polyethylene (HDPE) outer jacket. A total of ten samples were subjected to impulse testing under the same standardized procedure. The samples were immersed in insulating oil and connected between high-voltage and ground electrodes. Impulse voltages were applied in incremental steps until dielectric failure occurred, as confirmed by waveform collapse and post-test physical inspection.

Figure 45 shows a Cable C sample mounted and immersed in the test tank. After breakdown, visible carbonization and blackening are clearly seen around the midpoint, close to the grounding loop, consistent with a surface-initiated failure.

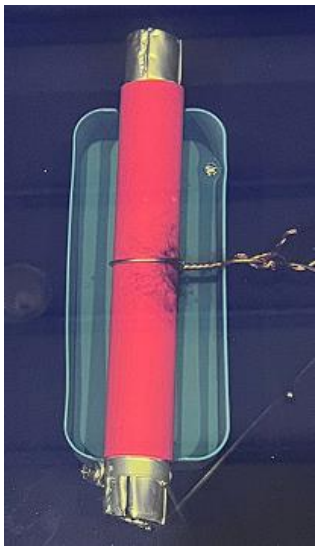

Figure 45: Cable C sample immediately after breakdown.

Following each breakdown event, the sample was retrieved and examined under light for visible jacket damage. Most failures in Cable C resulted in small, dark, circular puncture sites consistent with internal flashover. Figure 46 presents two examples of such markings, showing localized damage zones aligned with the waveform data.

Figure 46: Visible breakdown jacket markings in Cable C.

Oscillograph traces confirm distinct breakdown events for all tested samples. Figure 47 shows two representative breakdown waveforms from Samples 3 and 8. The negative peak voltages at which the impulse failed the cable were measured at approximately −75,1 kV and −79,9 kV, respectively, with a rapid voltage collapse and mild oscillation following the puncture.

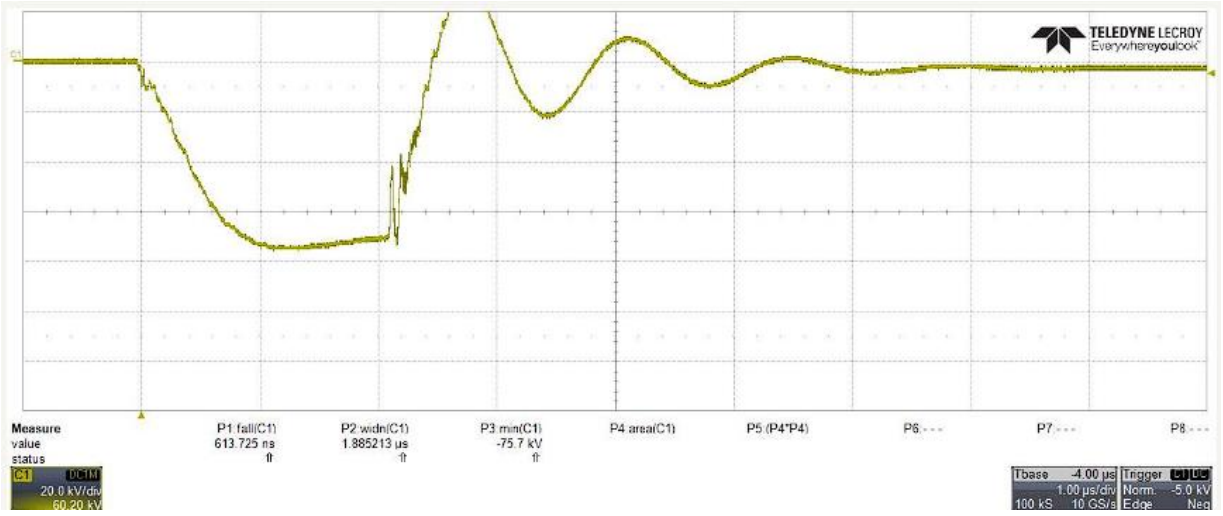

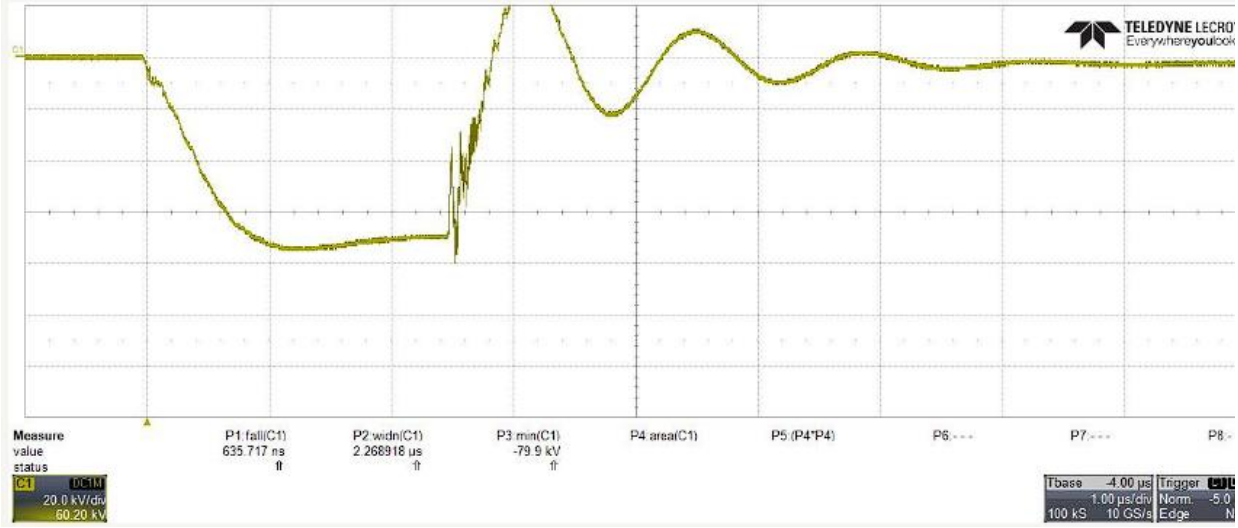

Figure 47: Oscillograph of impulse breakdown event for Sample 3 of Cable C(up) and oscillograph of impulse breakdown event for Sample 8 of Cable C(down).

The breakdown voltages for all ten samples are summarized in Table 20. The data span from −69,0 kV to −79,8 kV, indicating a slightly wider range of failure voltages. While the majority of samples failed around −72 to −75 kV, a few of them experienced earlier breakdown, suggesting the presence of localized jacket weaknesses or geometric field intensification.

Table 20: Breakdown voltage per sample for Cable Type C.

Breakdown Voltage per Sample	**Voltage (kV)**
Sample 1	-72,6
Sample 2	-74,2
Sample 3	-71,4
Sample 4	-72,6
Sample 5	-79
Sample 6	-72,6
Sample 7	-69
Sample 8	-70,2
Sample 9	-69
Sample 10	-79,8

3.6.4 Cable Type D: 20kV, AL-PE, MDPE

Cable Type D was constructed with an aluminum conductor, polyethylene insulation, and a medium-density polyethylene (MDPE) outer jacket. Ten Cable D samples were subjected to standardized impulse voltage testing. Each sample was immersed in insulating oil, connected to the high-voltage and ground electrodes via copper loops, and tested using increasing voltage steps until dielectric failure was observed. Visual inspection and oscilloscope trace analysis were used

to confirm breakdown occurrences. Figure 48 shows a Cable D sample immediately after breakdown within the oil tank. The discoloration and bubble trails near the center suggest energy release and jacket puncture during the discharge event, located near the ground connection.

Figure 48: Cable D sample immediately after breakdown.

Post-test examination of each sample revealed visible breakdown markings, typically appearing as small, circular burn spots or puncture sites on the jacket surface. These were used to correlate with oscilloscope data for accurate failure confirmation. Two examples are presented below.

Figure 49: Visible breakdown jacket markings in Cable D.

Representative voltage waveforms are shown in Figure 50 for Samples 5 and 7. In both cases, a sudden collapse of the negative voltage is followed by damped oscillations, confirming impulse-induced jacket failure.

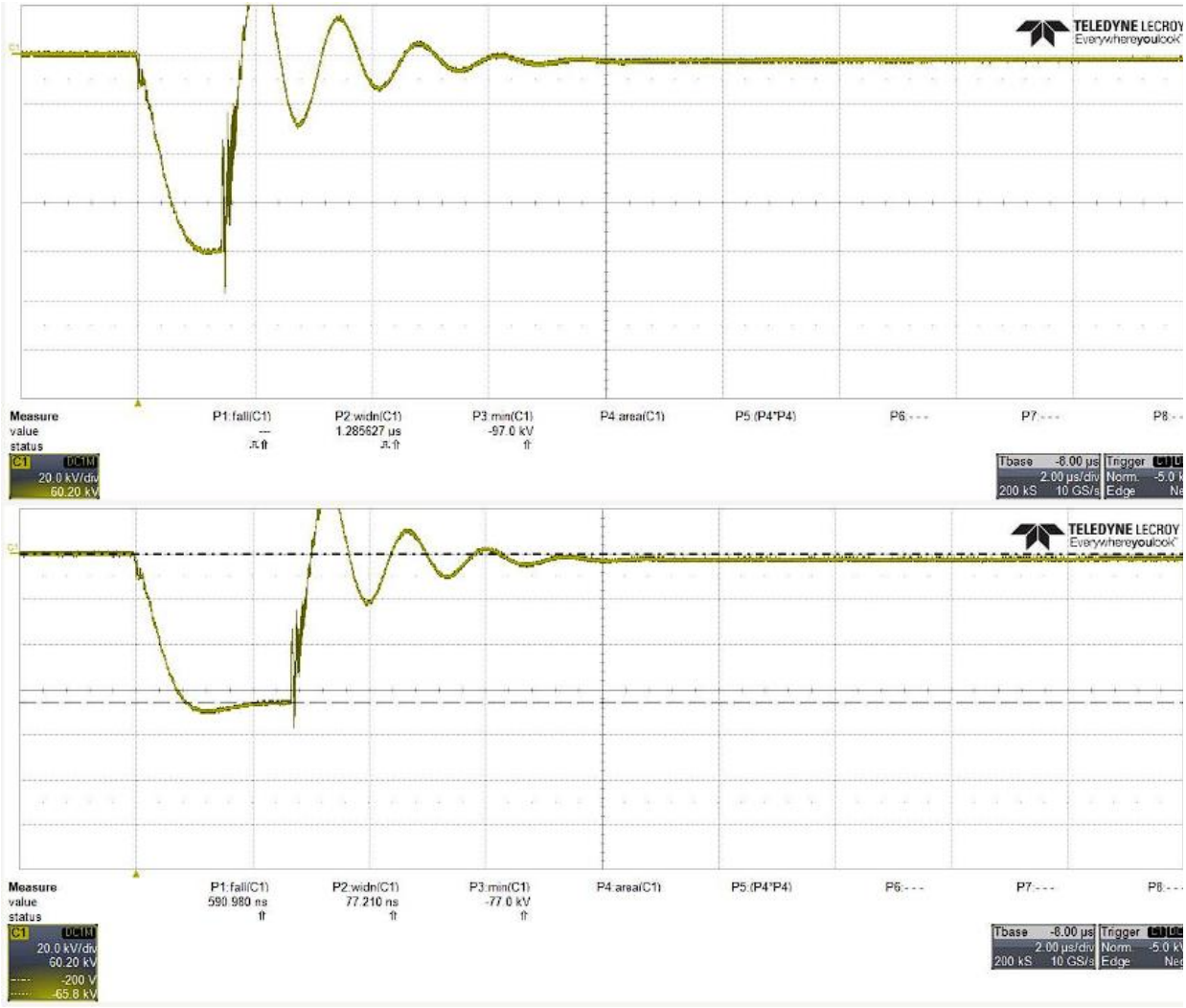

Figure 50: Oscillograph of impulse breakdown event for Sample 5 of Cable D(up) and oscillograph of impulse breakdown event for Sample 7 of Cable D(down).

The full set of breakdown voltages for Cable D is provided in Table 21.The results range from −65,8 kV to −80,0 kV, with most values clustered around −70 kV to −76 kV. This distribution shows relatively consistent behavior with only moderate variability.

Table 21: Breakdown voltage per sample for Cable Type D.

Breakdown Voltage per Sample	**Voltage (kV)**
Sample 1	-66,1
Sample 2	-76,2
Sample 3	-74,4
Sample 4	-66,1
Sample 5	-80
Sample 6	-76,5
Sample 7	-65,8
Sample 8	-66,7
Sample 9	-70,1
Sample 10	-72,8

3.6.5 Cable Type E: 1 kV, XLPE,SWA,PVC

Cable Type E differs significantly from the other samples in this study, as it is a low-voltage (1 kV-rated) power cable with a cross-linked polyethylene (XLPE) insulation, steel wire armour (SWA), and a PVC outer jacket. Despite its lower voltage rating, it was included in the test series to evaluate its jacket's ability to withstand high-voltage impulses and assess the dielectric strength margin compared to medium-voltage cables.

A total of ten samples were tested under the same stepwise impulse voltage procedure. The cables were immersed in mineral oil, mounted with copper wire loops at high-voltage and ground terminals, and subjected to increasing impulses until breakdown was visually and electrically confirmed. Figure 51 shows the aftermath of an impulse breakdown on one of the Cable E samples. A small but visible hole can be observed on the surface of the black PVC jacket, confirming the site of dielectric failure.

Figure 51: Visible breakdown jacket marking in Cable E.

Oscillograph data for two of the breakdown events are shown in Figure 49. Both waveforms exhibit a rapid voltage drop followed by partial recovery and oscillation, consistent with PVC jacket failure under high-voltage stress. Given the cable's low nominal voltage rating (1 kV), these impulse withstand levels are relatively high but not unexpected, as the jacket is not normally designed to handle such transients.

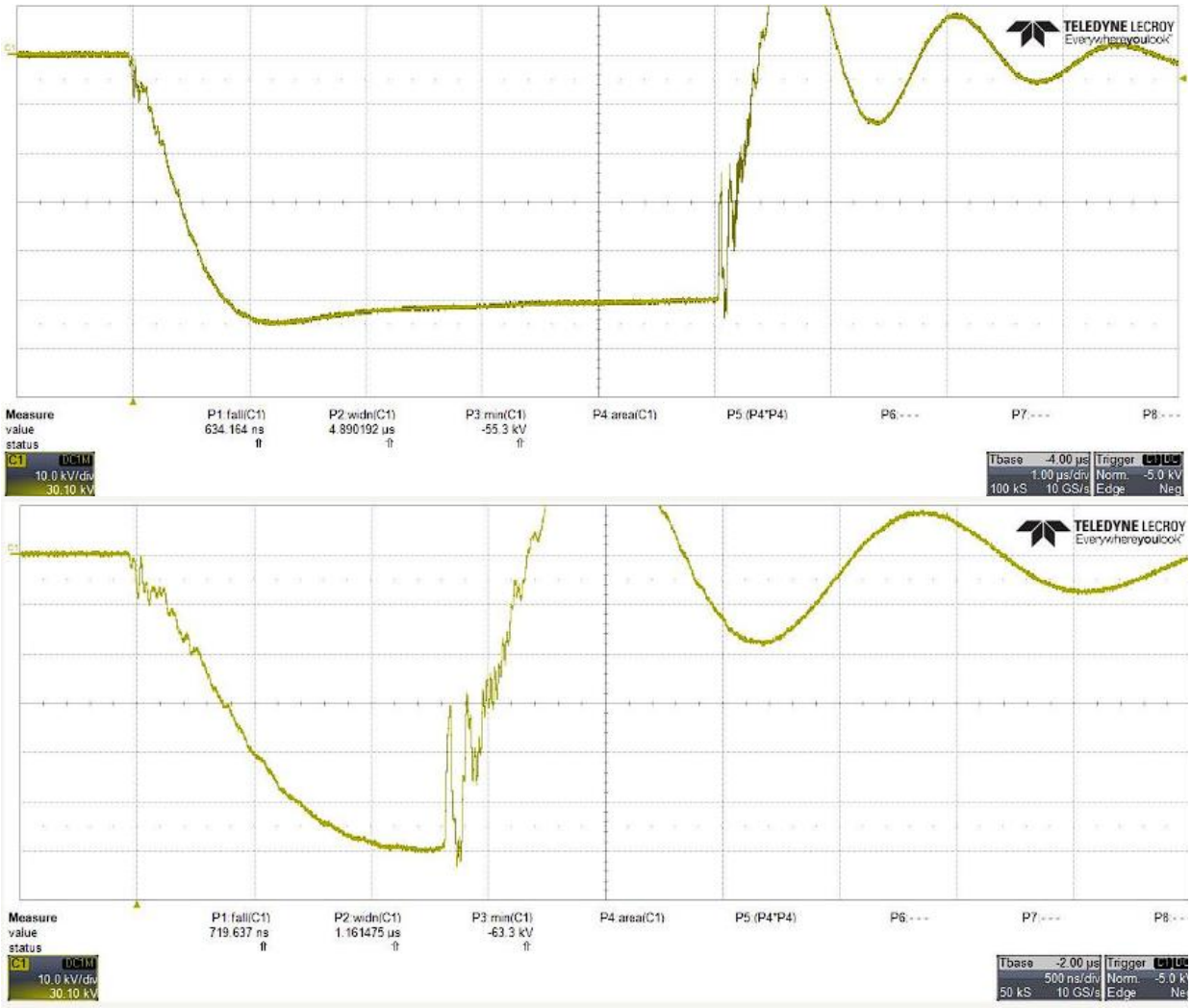

Figure 52: Oscillograph of impulse breakdown event for Sample 4 of Cable E(up) and oscillograph of impulse breakdown event for Sample 10 of Cable E(down).

The breakdown voltages for all ten samples are presented in Table 22. The range spans from −40,0 kV to −60,2 kV, indicating significant variation. This variability could stem from inconsistent jacket thickness or inherent PVC aging and material sensitivity.

Table 22: Breakdown voltage per sample for Cable Type E.

Breakdown Voltage per Sample	**Voltage (kV)**
Sample 1	-57,5
Sample 2	-59,3
Sample 3	-51,1
Sample 4	-50,2
Sample 5	-51,2
Sample 6	-60,2
Sample 7	-56,8
Sample 8	-60,2
Sample 9	-40
Sample 10	-59,8

CHAPTER 4: STATISTICAL ANALYSIS OF BREAKDOWN VOLTAGE RESULTS

This chapter presents a statistical analysis of the experiment results obtained during impulse testing of medium voltage cable samples. The aim is to characterize the dielectric strength of each cable by determining key statistical breakdown voltage values and by evaluating the breakdown performance in terms of thickness-normalized electric field strength (kV/mm), offering a more intrinsic measure of dielectric capability independent of physical dimensions.

4.1 Percentile Analysis of Breakdown Voltage

Percentile-based breakdown voltages serve as statistical indicators when it comes to disruptive discharge voltage values. Specifically, the p% disruptive-discharge voltage U_p is defined as the prospective voltage which has a probability p of producing a disruptive discharge on the test object. Conversely, the withstand voltage is the voltage level below which the test object is expected to survive without breakdown with a probability of [13]:

$$q = 1 - p \qquad (4)$$

The key values of the statistical are:

- $U_{10\%}$: the voltage which 10% of samples will break down, also referred to as the statistical withstand voltage [13].
- $U_{50\%}$: the voltage at which 50% of the samples are expected to fail under test conditions. This value corresponds to the Critical Flashover Voltage (CFO) or median breakdown voltage [26].
- $U_{90\%}$: the voltage below which 90% of the tested samples are expected to fail. It is sometimes referred to as the statistical assured disruptive-discharge voltage [13].

In insulating material testing, the breakdown voltage is typically determined by gradually increasing the applied voltage, either in steps or using a linear ramp, until failure occurs. Each

sample's breakdown point reflects the random nature of dielectric failure, influenced by microscopic defects and material variability [27]. The breakdown point for each sample is inherently stochastic, influenced by micro-defects, material inconsistencies, and localized electric field intensification [27]. To account for this probabilistic behavior, the Generalized Extreme Value (GEV) distribution is employed for modeling breakdown voltages.

The GEV distribution unifies three types of extreme value distributions, Gumbel, Fréchet, and reverse Weibull, and is particularly suitable for modeling the statistical extremes of dielectric failure. Its cumulative distribution function (CDF) is expressed as:

$$F(V) = exp\left\{-\left[1 + \xi\left(\frac{V-\mu}{\sigma}\right)^{-1/\xi}\right]\right\} \quad (5)$$

Here, V is the breakdown voltage in kV, μ is the location parameter (analogous to the center of the distribution), σ is the scale parameter, and ξ is the shape parameter that determines the tail behavior of the distribution. The sign and magnitude of ξ define the type of distribution:

- $\xi>0$: Fréchet-type (polynomial tail)
- $\xi=0$: Gumbel-type (exponential tail)
- $\xi<0$: reverse Weibull-type (upper bounded tail)

After fitting the GEV distribution to the experimental data, the inverse of the cumulative distribution function is used to compute key percentile values such as U_{10}, U_{50} and U_{90}. The quantile function for the GEV distribution is given by:

$$U_p = \mu + \frac{\sigma}{\xi}[(-ln\, p)^{-\xi} - 1] \quad (6)$$

The parameters μ, σ, and ξ were estimated from the measured breakdown voltage data using MATLAB's built-in gevfit function, which performs maximum likelihood estimation (MLE) for the GEV model. For each cable type, the resulting GEV parameters were used to extract statistical breakdown voltages at specified probability levels.

Using MATLAB, GEV-based percentile plots were generated for each cable type to visualize the fit against the measured breakdown voltages. Each curve was validated by plotting the empirical data and confirming that the estimated percentile values closely align with the analytical

predictions. In particular, the U_{10}, U_{50}, and U_{90} breakdown voltages serve as critical indicators of dielectric reliability under transient stress conditions.

NOTE: Although the breakdown voltages measured in the experiment were negative due to applied polarity, all values reported in the GEV analysis are presented in absolute terms, in accordance with standard reliability modeling practices.

4.1.1 Cable Type A: NA2XSY 20kV, CWS, PVC

For Cable Type A (NA2XSY 20 kV, CWS, PVC), the GEV analysis yielded a shape parameter of $\xi = -1{,}16$, a scale parameter of $\sigma = 2{,}32$kV, and a location parameter of $\mu = 64.69$ kV. The negative shape parameter indicates a Weibull-type (bounded tail) distribution within the GEV family, suggesting a statistically bounded upper limit for breakdown voltages. This form is consistent with dielectric systems that exhibit a maximum strength threshold, beyond which breakdown is physically implausible due to material constraints.

The computed percentile thresholds were $U_{10} = 61{,}4$ kV, $U_{50} = 65{,}4$ kV, and $U_{90} = 66{,}6$ kV, corresponding to the breakdown voltages at which 10%, 50%, and 90% of the tested specimens are expected to fail under impulse conditions. The spread between U_{10} and U_{90} is relatively narrow, approximately 5.2 kV, indicating a concentrated failure region and suggesting uniform electrical properties across the tested population.

Despite the small sample size, the fitted GEV curve exhibits good visual agreement with the empirical data. The plotted sample points lie close to the theoretical curve, especially in the mid-to-upper percentiles, reinforcing the appropriateness of the GEV model for this dataset. Notably, the sharp curvature in the upper region of the probability plot reflects the steep increase in failure likelihood as voltage approaches the statistical maximum, which is consistent with a negative shape parameter and a well-manufactured insulating jacket with minimal outliers.

Overall, Cable Type A demonstrates consistent dielectric behavior and a bounded, statistically robust breakdown profile under standardized impulse stress. The results support the classification of this cable as reliable for medium-voltage applications, particularly in environments where overvoltage resilience and manufacturing consistency are critical.

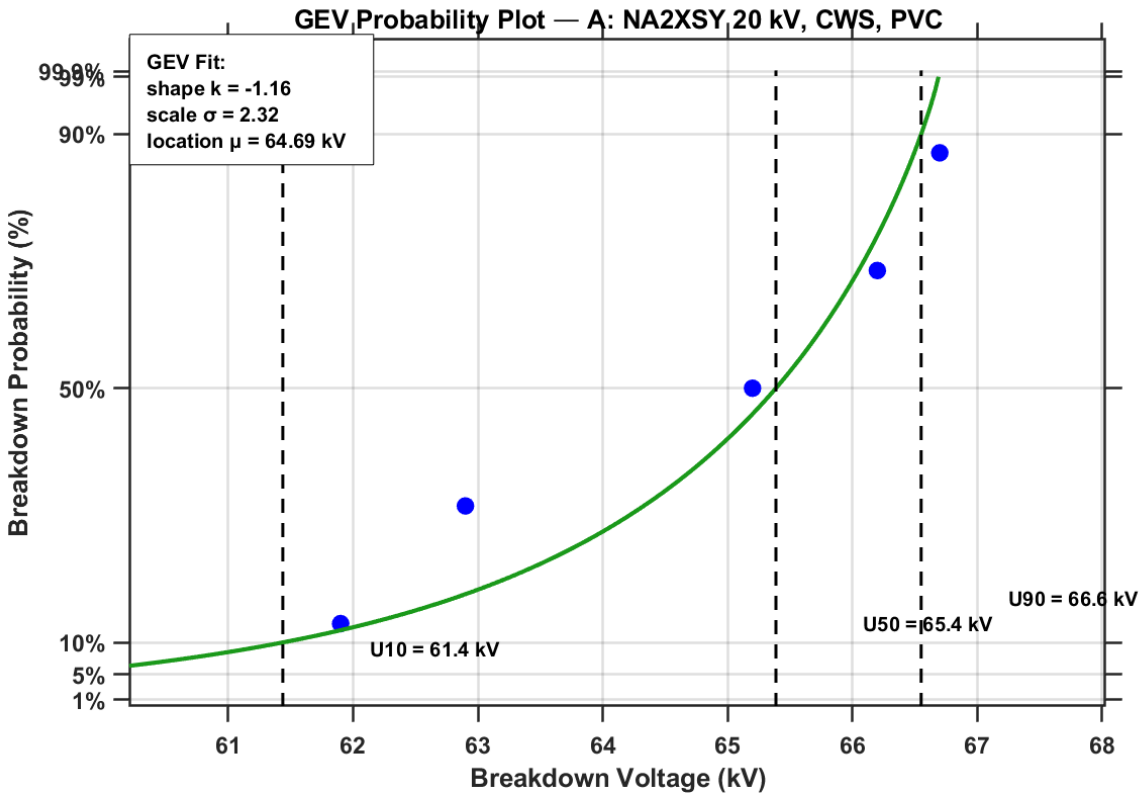

Figure 53: GEV probability plot for Cable A (NA2XSY 20 kV, CWS, PVC).

4.1.2 Cable Type B: 20kV, CWS, PPS+HDPE

For Cable Type B (20 kV, CWS, PPS+HDPE), the GEV fit produced a shape parameter of $\xi = -0{,}49$, a scale parameter of $\sigma = 2{,}90$ kV, and a location parameter of $\mu = 73{,}51$kV. The negative shape parameter again indicates a bounded Weibull-type distribution within the GEV framework, but with a much gentler curvature compared to Cable A, reflecting a broader, but still controlled, range of failure voltages.

The calculated breakdown thresholds were $U_{10} = 70{,}5$ kV, $U_{50} = 74{,}5$ kV, and $U_{90} = 77{,}5$ kV, yielding a percentile spread of just 7,0 kV. This relatively narrow band, especially across a larger sample size of ten specimens, reinforces the strong manufacturing uniformity and dielectric reliability of the tested jacket material. The breakdown voltages are not only statistically consistent but also significantly elevated relative to the cable's nominal voltage class, suggesting robust overvoltage tolerance.

Visually, the GEV model exhibits a particularly good fit to the empirical data, with nearly all sample points aligning smoothly with the theoretical distribution curve. The consistent rise in breakdown probability across voltages is captured without notable outliers or deviation, indicating that the electrical failure characteristics of this cable are well-behaved and appropriately modeled by the GEV distribution.

The use of a composite PPS+HDPE jacket in Cable B appears to confer distinct advantages under impulse conditions. Not only are the breakdown voltages high, but their tight clustering around the median implies that performance is predictable and dependable. Among all the tested cables, Cable B emerges as one of the most statistically robust candidates, ideally suited for installations where exposure to impulse stress or lightning surges is a critical design consideration.

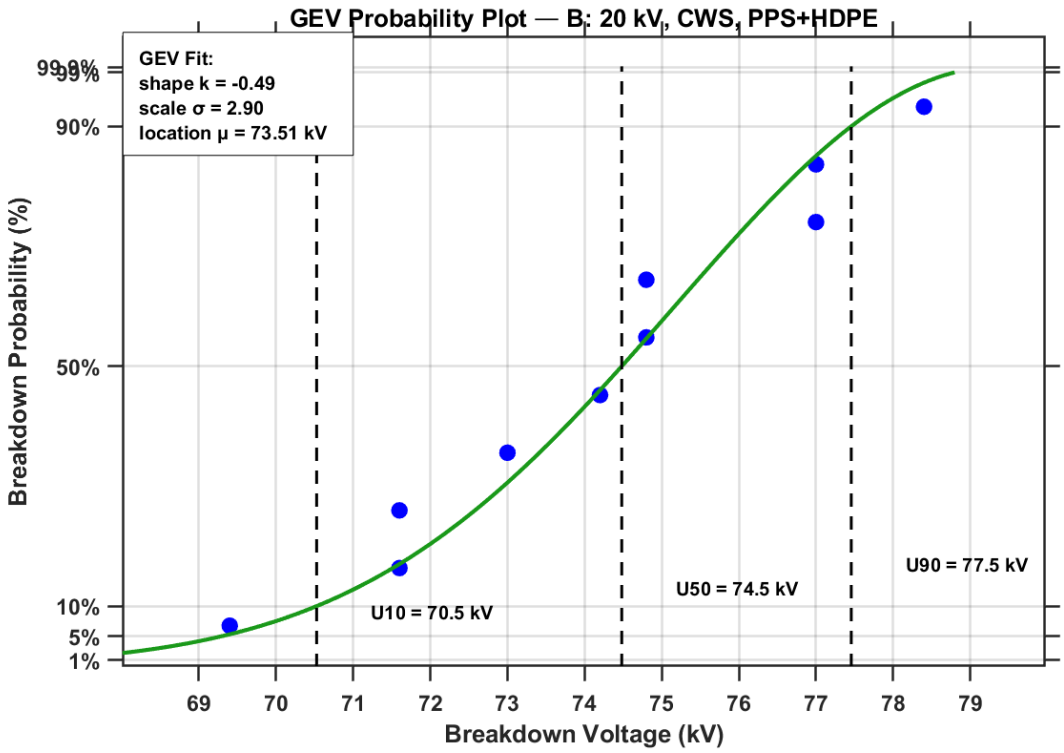

Figure 54: GEV probability plot for Cable B (20kV, CWS, PPS+HDPE).

4.1.3 Cable Type C: 20kV, AL-PE, HDPE

For Cable Type C (20 kV, AL-PE, HDPE), the GEV analysis resulted in a shape parameter of ξ=0,20, a scale parameter of σ=2,39, and a location parameter of μ=71,16kV. The positive value of the shape parameter indicates a Fréchet-type distribution, which is associated with a heavier

upper tail. This suggests that, while most breakdown voltages are concentrated around the median, there is a higher probability of observing values significantly above the central tendency.

The computed GEV percentile thresholds were U_{10}=69,3 kV, U_{50}= 72,1 kV, and U_{90}=77,9 kV, resulting in a span of 8,6 kV between the 10th and 90th percentiles. This range is slightly broader than that of Cable B, reflecting a modest increase in variability among the breakdown measurements. However, the distribution remains well-structured, with no indication of extreme outliers or premature failures.

The green GEV fit curve aligns well with the empirical data across the probability scale, although a mild scatter is visible in the central region, suggesting slightly less uniformity compared to Cable B. Still, the overall distribution maintains statistical coherence, and the deviation from the fit remains within acceptable limits for practical applications. The median breakdown voltage of 72,1 kV lies comfortably above the nominal stress level for the 20 kV cable class, supporting the suitability of the HDPE jacket material for high-voltage environments.

In conclusion, Cable Type C demonstrates reliable impulse withstand capability with slightly broader statistical dispersion, likely attributable to normal manufacturing variability such as surface roughness, jacket thickness variation, or microscopic defects. The GEV analysis confirms that the breakdown behavior is well modeled, with no anomalous trends. Overall, Cable C performs solidly, with predictable dielectric characteristics under transient overvoltage conditions.

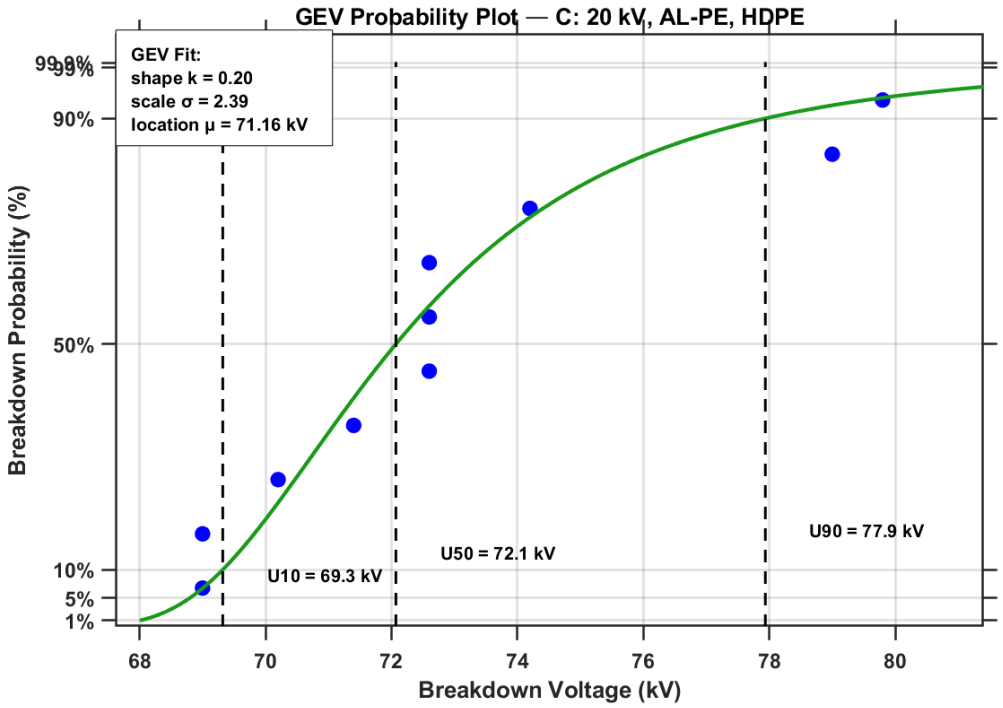

Figure 55: GEV probability plot for Cable C (20kV, AL-PE, HDPE).

4.1.4 Cable Type D: 20kV, AL-PE, MDPE

For Cable Type D (20 kV, AL-PE, MDPE), the GEV statistical analysis produced a shape parameter of $\xi = -0{,}14$, a scale parameter of $\sigma = 4{,}39$, and a location parameter of $\mu = 69{,}38$kV. The slightly negative shape parameter indicates a light Weibull-type distribution, suggesting a finite upper bound for breakdown strength while allowing moderate variability in the lower percentiles.

The computed percentile values were $U_{10} = 65{,}5$ kV, $U_{50} = 70{,}9$ kV, and $U_{90} = 77{,}9$ kV, resulting in a relatively wide spread of 12,4 kV between the 10th and 90th percentiles. This broader range, compared to the other cable types, points to a greater level of statistical dispersion across the tested specimens, particularly in the lower tail of the distribution.

The GEV fit curve (green) follows the general trend of the data well, but increased scatter is evident among the empirical points, especially in the 10% to 50% probability region. Several samples show early breakdown behavior between 65 and 68 kV, which lowers the U_{10} value and slightly flattens the slope of the cumulative probability curve. This behavior could be attributed to variations in extrusion quality, material homogeneity, or minor defects in the MDPE jacket.

Despite this, the median breakdown voltage of 70,9 kV remains well above the nominal class rating, indicating good average dielectric strength. The statistical profile of Cable D suggests that while its insulation system is fundamentally reliable, it may benefit from tighter quality control to reduce early failures and compress the lower tail of the distribution.

In conclusion, Cable Type D demonstrates satisfactory impulse performance for medium-voltage applications, with a robust characteristic breakdown level but somewhat elevated variability. The GEV model captures this behavior well, highlighting the cable's practical reliability alongside opportunities for manufacturing refinement.

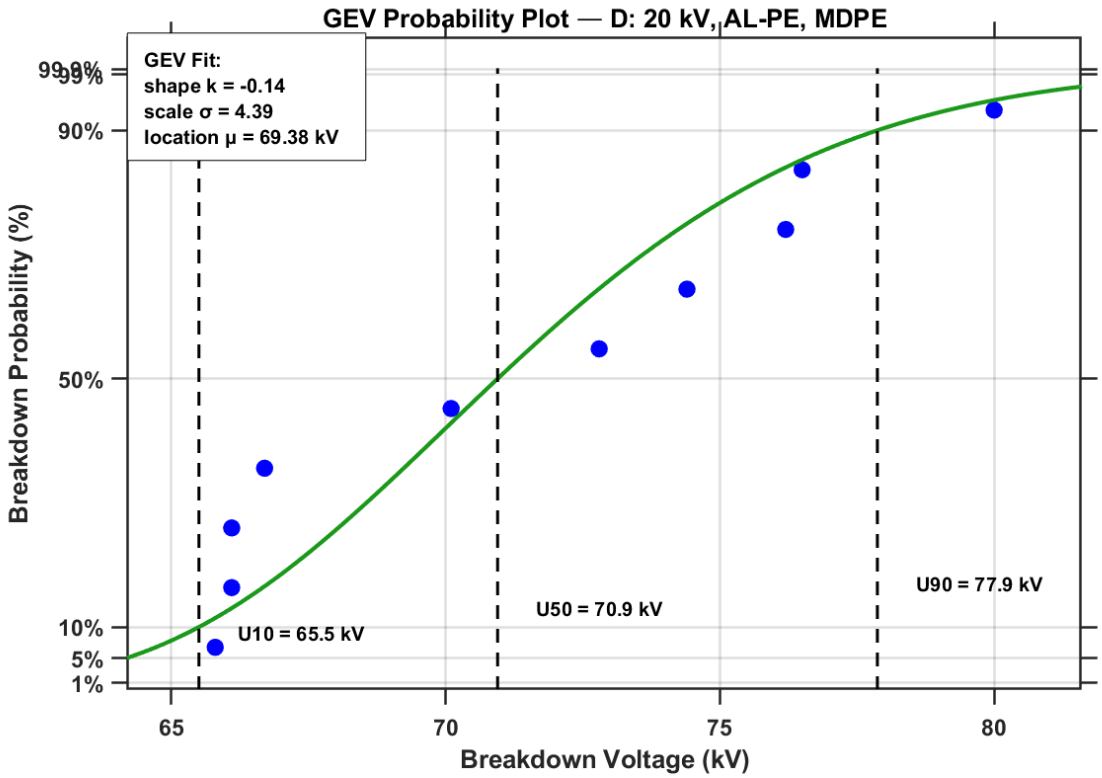

Figure 56: GEV probability plot for Cable D (20kV, AL-PE, MDPE).

4.1.5 Cable Type E: 1 kV, XLPE,SWA,PVC

For Cable Type E (1 kV, XLPE, SWA, PVC), the GEV analysis reveals a significantly different breakdown behavior compared to the higher-rated medium voltage cables. The fitted distribution yielded a shape parameter of $\xi = -1{,}26$, a scale parameter of $\sigma = 6{,}67$, and a location parameter of

μ=54,91kV. The strongly negative shape value indicates a bounded Weibull-type distribution with a sharp cutoff, consistent with a physical upper limit to the jacket's dielectric strength.

The estimated percentile breakdown voltages were U_{10}=45,1 kV, U_{50}= 56,9 kV, and U_{90}=59,9 kV, yielding a spread of 14,8 kV between the 10th and 90th percentiles, the widest among all tested cable types. This broad range indicates pronounced statistical variability, with several early failures pulling down the lower tail of the distribution. Such dispersion may arise from inconsistencies in material quality, surface imperfections, or sensitivity to mechanical damage introduced during sample handling.

Despite these variations, the fitted GEV curve closely follows the empirical data and provides a statistically meaningful representation of the cable's behavior. The median breakdown voltage U_{50} of 56,9 kV demonstrates that the PVC jacket significantly exceeds its nominal 1 kV rating under impulse stress, offering a considerable dielectric safety margin. However, the lower bound of performance, represented by U_{10}, reveals that a subset of samples may fail prematurely, potentially limiting the reliability of this cable under severe transient conditions.

In summary, Cable Type E exhibits a high absolute dielectric strength for its class but also demonstrates the greatest variability among the tested cables. While its impulse performance is notable, the broader percentile distribution and early breakdown instances suggest that further optimization of material formulation or processing may be necessary to enhance consistency and reduce the risk of early failures in practical applications.

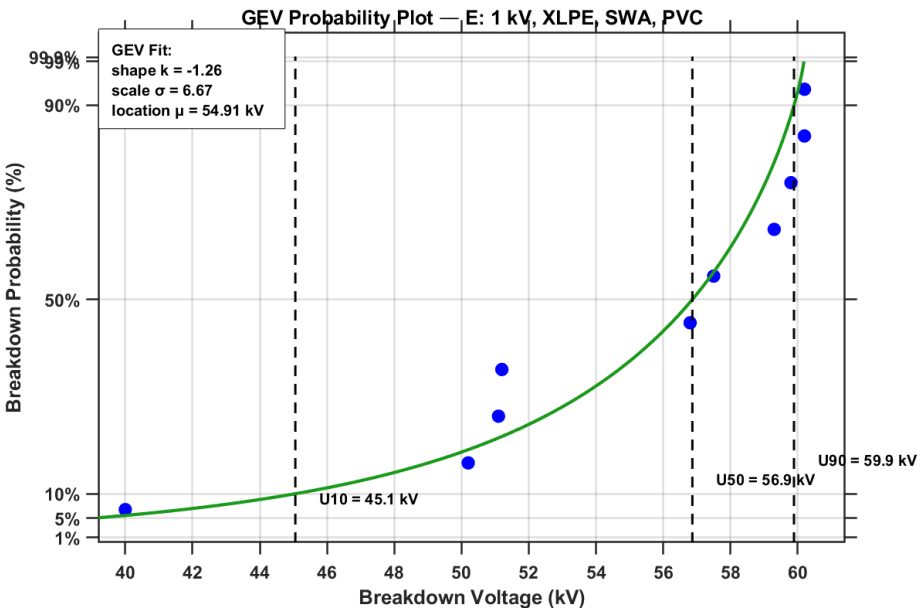

Figure 57: GEV probability plot for Cable E (1 kV, XLPE, SWA, PVC).

Table 23 summarizes the statistical percentiles obtained:

Table 23:GEV percentile breakdown voltages (U_{10}, U_{50}, U_{90}) per cable type.

Cable Type	**U_{10} (kV)**	**U_{50} (kV)**	**U_{90} (kV)**
Cable Type A: NA2XSY 20kV, CWS, PVC	61,4	65,4	66,6
Cable Type B: 20kV, CWS, PPS+HDPE	70,5	74,5	77,5
Cable Type C: 20kV, AL-PE, HDPE	69,3	72,1	77,9
Cable Type D: 20kV, AL-PE, MDPE	65,5	70,9	77,9
Cable Type E: 1 kV, XLPE, SWA, PVC	45,1	56,9	59,9

Despite differences in rated voltage and construction, the impulse breakdown behavior of the five cable types can be compared using the spread between their 10th and 90th percentile voltages (U_{10}–U_{90}). Cable Type A exhibits the narrowest spread at 5,2 kV, indicating low statistical variability; however, this result should be interpreted with caution as it is based on only half the number of samples tested compared to the other cables, which limits its statistical robustness. Cable Type B, tested with a full sample set, shows the next narrowest spread at 7,0 kV, reflecting highly consistent dielectric performance and reliable manufacturing. Cables C and D display intermediate variability, with spreads of 8,6 kV and 12,4 kV respectively, while Cable Type E shows the widest spread at 14,8 kV, suggesting greater inconsistency despite its relatively strong absolute breakdown strength. Overall, narrower percentile ranges point to more predictable insulation behavior under impulse stress, with Cable B standing out as the most statistically reliable among those with a complete dataset.

Table 24: GEV Parameters Table.

Cable Type	**Shape parameter – k**	**scale parameter – σ**	**Location parameter (kV)**
Cable Type A: NA2XSY 20kV, CWS, PVC	-1,16	2,32	64,69
Cable Type B: 20kV, CWS, PPS+HDPE	-0,49	2,90	73,51
Cable Type C: 20kV, AL-PE, HDPE	0,20	2,39	71,16
Cable Type D: 20kV, AL-PE, MDPE	-0,14	4,39	69,38
Cable Type E: 1 kV, XLPE, SWA, PVC	-1,26	6,67	54,91

Table 24 presents the GEV distribution parameters for all tested cable types, providing a comparative perspective on their dielectric performance under impulse stress. The location parameter μ represents the central tendency or typical breakdown voltage, while the scale parameter σ reflects the spread or variability of the distribution. The shape parameter ξ defines the

tail behavior, with negative values indicating a bounded upper limit and positive values suggesting heavier tails. Cable Type B shows the highest location parameter (μ=73,51) and a relatively small scale (σ=2,90), indicating both strong and consistent dielectric performance. In contrast, Cable Type E exhibits the lowest location (μ=54,91) and the largest scale (σ=6,67), highlighting its comparatively weaker insulation strength and greater statistical variability. These GEV parameters clearly differentiate the breakdown behavior of the tested cable jackets and underscore the impact of material composition and construction quality on high-voltage reliability.

4.2 Thickness-Normalized Breakdown Field Strength (kV/mm) Analysis

The dielectric strength of cable jackets is a critical parameter in assessing their ability to withstand high-voltage impulse events without insulation failure. However, comparing absolute breakdown voltages across cables of varying dimensions may obscure meaningful patterns in material performance. To address this limitation, the present analysis expresses breakdown behavior in terms of electric field strength per unit thickness, defined as:

$$E_{BD} = \frac{|V_{BD}|}{d} \quad \left(\frac{kV}{mm}\right) \tag{7}$$

Where E_{BD} is the electric breakdown strength, V_{BD} is the absolute value of the breakdown voltage and d is the average thickness of the outer insulating layer. This thickness-normalized parameter reflects the material's ability to withstand electric stress independent of geometric dimensions, thereby enabling a more objective comparison across different cable types [28].

In accordance with established testing practices for solid insulating materials under high-voltage stress, this methodology enables a more representative evaluation of a material's dielectric endurance. It reflects both the electric field strength required to initiate breakdown and the inherent variability due to geometric or manufacturing factors [10].

To implement this analysis, MATLAB was used to normalize the breakdown voltage values collected from impulse testing of five different MV cable types. By dividing each sample's breakdown voltage by the corresponding average jacket thickness, a normalized electric field strength (in kV/mm) was calculated, enabling a more representative assessment of the dielectric endurance of each insulation system. The results were then subjected to basic statistical analysis,

including the calculation of the mean, standard deviation, and coefficient of variation (CV) for the breakdown field strength.

Table 25 presents the results obtained from the MATLAB analysis of the breakdown field strength for each cable type. The mean value indicates the typical electric stress level that the jacket can handle before breaking down. The standard deviation shows how much the individual values differ from the average, giving an idea of the consistency within each cable type. The coefficient of variation (CV) expresses this variation as a percentage of the mean, making it easier to compare how consistent the results are across different cable types. These three values together help evaluate both the average strength and the reliability of each cable jacket.

Table 25: Statistics of breakdown field strength (kV/mm) across cable types, normalized by average jacket thickness.

Cable Type	**Thickness**	**Mean E (kV/mm)**	**Std E (kV/mm)**	**CV (%)**
A: NA2XSY 20 kV, CWS, PVC	2,30	28,08	0,91	3,2
B: 20 kV, CWS, PPS+HDPE	2,40	30,91	1,18	3,8
C: 20 kV, AL-PE, HDPE	2,50	29,22	1,50	5,1
D: 20 kV, AL-PE, MDPE	2,30	31,07	2,27	7,3
E: 1 kV, XLPE, SWA, PVC	2,40	21,85	2,60	11,9

From the statistical summary, Cable Types B and D demonstrate the highest average breakdown field strengths, with mean values of 30,91 kV/mm and 31,07 kV/mm, respectively. These results suggest superior jacket properties, likely attributed to the use of engineered materials such as PPS+HDPE and MDPE, which are known for their electrical characteristics under high-voltage stress. In contrast, Cable Type E, which is a 1 kV-rated construction incorporating PVC, yielded the lowest mean field strength at 21,85 kV/mm. This substantial difference reinforces the influence of both material selection and voltage class on dielectric performance. The scatter plot

in Figure 58 complements these findings by illustrating the full distribution of normalized breakdown values per sample.

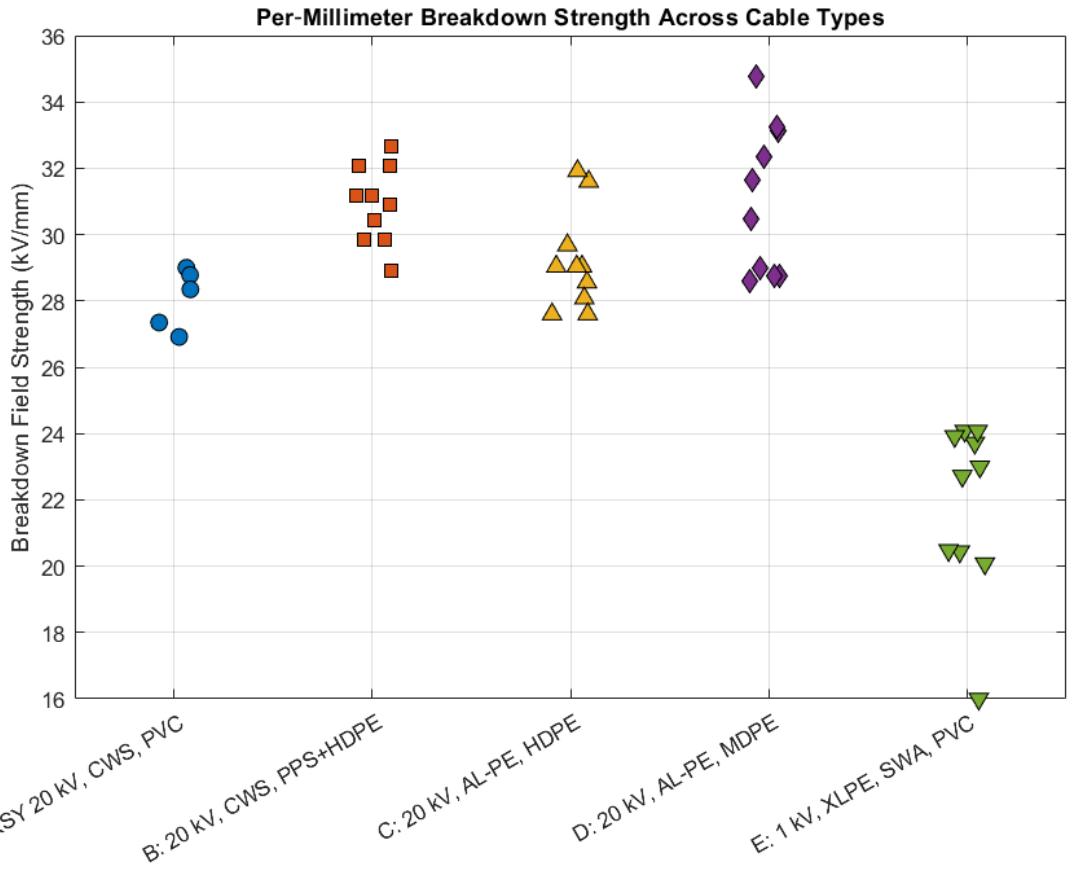

Figure 58: Per-sample breakdown field strength (kV/mm) of each cable type derived by normalizing impulse breakdown voltage with jacket thickness.

The breakdown field strength values for Cable Type A demonstrate moderate dielectric performance, with all measurements falling within a narrow range of approximately 27 to 29 kV/mm. This clustering indicates relatively uniform behavior across the tested samples. The coefficient of variation (CV) is 3,2%, the lowest among all cable types, suggesting high consistency and minimal dispersion. The absence of significant outliers implies good manufacturing quality and stable jacket performance under impulse stress.

Cable Type B demonstrates the most consistent dielectric performance across all tested cables. Breakdown field strength values are tightly packed between approximately 29 and 33 kV/mm, with no visible outliers. This tight clustering corresponds to an exceptionally low coefficient of variation (3,8%) and suggests a high-quality insulation system with uniform properties. The

combination of PPS and HDPE as outer jacket materials appears to deliver exceptionally reliable protection under impulse stress.

For Cable Type C, the results show stable but slightly lower field strength values, ranging from 28 to 32 kV/mm. While the performance is still good, the measurements exhibit a slightly wider spread and a higher coefficient of variation (5,1%). This contributes to a material system that performs reliably but may be somewhat more affected by minor inconsistencies in thickness or material composition.

Cable Type D records the highest mean breakdown field strength of all groups, with values reaching up to nearly 35 kV/mm. Most samples cluster between 29 and 34 kV/mm, showing strong dielectric endurance. However, the variability is slightly higher than in Type B, as reflected by a coefficient variation of 7,3%. This suggests that while the MDPE-based outer jacket provides excellent protection, its consistency may not match that of the PPS+HDPE formulation.

In contrast, Cable Type E exhibits the lowest breakdown field strength values, ranging mostly between 20 and 24 kV/mm, with a minimum of just 16 kV/mm. The relatively low mean and broad spread (CV=11,9%) suggest a less robust dielectric performance, likely due to its lower voltage rating and different structural design.

Overall, the analysis of breakdown field strength provides important insight into the electrical reliability of different cable designs. By normalizing breakdown voltage with respect to jacket thickness, a clearer picture emerges of how each material performs under comparable stress conditions. The results highlight not only the average strength of each cable type, but also how consistently that performance is achieved across samples.

4.3 Breakdown Timing During Impulse Waveform

Impulse voltage testing is a widely adopted method for assessing the dielectric strength of cable insulation systems under transient overvoltage conditions. In most applications, the main focus lies in determining the breakdown voltage. However, this approach alone does not fully reflect the dynamic nature of dielectric failure. When testing with standardized lightning impulse waveforms, the timing of breakdown along the waveform is also a parameter of considerable diagnostic value.

The applied impulses in this study follow the 1,2/50 μs waveform specification, with negative polarity. The waveform begins at zero, rapidly drops to a negative peak within approximately 1,2 μs (front time), and then gradually recovers toward zero over a period of about 50 μs (tail time). Dielectric breakdown, observed as a sudden collapse in voltage, can occur at any point along this waveform, during the steep front, near the peak, or on the decaying tail. Each of these regions corresponds to different stress conditions acting on the material, and consequently, different failure mechanisms [13], [29].

Breakdowns occurring during the initial microseconds of the impulse are typically associated with high voltage gradients and fast-rising electric fields. These early failures are often interpreted as field-driven phenomena. In contrast, failures that take place later in the waveform after the peak may be influenced by slower processes such as local charge accumulation, partial discharges, or thermal effects. In these cases, the material survives the peak field but eventually fails under sustained or delayed stress [29].

To further analyze the timing of dielectric failure under impulse conditions, a MATLAB script was implemented to classify each breakdown event based on when it occurred along the standardized 1,2/50 μs waveform. The standard front time of the applied 1,2/50 μs impulse, was selected as the reference point separating the early, fast-rising portion of the waveform from the later, gradually decaying region. Each breakdown event was categorized based on its recorded time: if the breakdown occurred at or before 1,2 μs, it was classified as a front wave failure; otherwise, it was considered a tail wave failure. For each cable type, the number of front and tail events was quantified, and the corresponding percentages were computed to assess the prevailing breakdown tendency. The complete breakdown time dataset for all tested samples is presented in Table 26.

Table 26: Breakdown time (μs) per sample for all cable types.

Breakdown Time per Sample (μs)	**Type A**	**Type B**	**Type C**	**Type D**	**Type E**
Sample 1	1,737	5,253	1,868	1,016	1,943
Sample 2	2,359	1,661	1,068	1,944	1,254
Sample 3	1,459	1,584	2,038	1,126	3,262
Sample 4	1,310	1,278	1,894	1,414	4,992
Sample 5	1,486	1,055	1,106	1,138	3,317
Sample 6		1,905	3,337	2,720	1,300
Sample 7		1,040	2,415	1,550	0,915
Sample 8		1,023	4,182	2,204	1,236
Sample 9		1,500	3,018	1,672	1,346
Sample 10		2,000	2,500	2,000	1,387

To summarize the classification results, Table 27 presents the number and percentage of breakdown events that occurred during the front (≤ 1,2 μs) and tail (> 1,2 μs) portions of the impulse waveform for each cable type. The data reveals a consistent tendency across all samples. Dielectric breakdowns occur predominantly after the impulse front, highlighting a tail region failure preference in the tested cable jackets.

Table 27: Front and Tail Breakdown Classification per Cable Type.

Cable Type	**Front Failures**	**Tail Failures**	**Front (%)**	**Tail (%)**	**Dominance**
A: NA2XSY 20 kV, CWS, PVC	0	5	0,0	100,0	Tail
B: 20 kV, CWS, PPS+HDPE	3	7	30,0	70,0	Tail
C: 20 kV, AL-PE, HDPE	2	8	20,0	80,0	Tail
D: 20 kV, AL-PE, MDPE	3	7	30,0	70,0	Tail
E: 1 kV, XLPE, SWA, PVC	1	9	10,0	90,0	Tail

Cable Sample A exhibited no breakdowns during the front of the impulse waveform, with all six failures occurring beyond the 1,2 μs threshold. The resulting 0% front and 100% tail classification confirms a strong resistance to high dV/dt conditions but a pronounced

vulnerability to delayed or cumulative stress effects. This behavior is consistent with thermally activated or space-charge-driven failure mechanisms.

For cable Sample B, three of ten breakdowns occurred within the front time, while the remaining seven occurred during the tail, yielding a 30% front and 70% tail distribution. Although this suggests partial sensitivity to rapid field rise, the predominant failure mode is clearly governed by post-peak dielectric stress, classifying the cable as tail dominant.

Cable Sample C showed a similar trend, with only two front-region failures out of ten, corresponding to 20% front and 80% tail breakdowns. The limited number of early failures implies a certain degree of front-time endurance, while the majority tail failures suggest that the insulating material is more susceptible to time-dependent deterioration mechanisms.

Cable Sample D also recorded three front region breakdowns and seven in the tail, matching the percentage distribution of Sample B (30% / 70%). This further supports the conclusion that the material properties or structural characteristics of this cable type predispose it to delayed failure rather than breakdown under the steep initial gradient.

Cable Sample E presented the most unbalanced profile among all groups, with just one breakdown occurring during the front time and nine in the tail. The resulting 10% front and 90% tail ratio demonstrates the greatest level of tail dominance in the study. This behavior suggests high front-time withstand capability, potentially attributable to the material's resistance to rapid electric field change, but a significant decline in endurance under sustained dielectric loading.

Collectively, the data reinforces the hypothesis that, for the tested jacket materials, impulse-induced breakdown is more commonly triggered under the slower, decaying tail of the waveform. This observation emphasizes the importance of evaluating not only the peak electric field but also the time-dependent behavior of insulating materials under standardized impulse conditions.

CHAPTER 5: CONCLUSION

5.1 Overview of the Study

This thesis explored the dielectric strength performance of various medium-voltage (MV) cable jackets when subjected to standardized 1,2/50 μs lightning impulse waveforms. The experimental work focused on outer sheath materials, assessing their ability to withstand fast transient overvoltages using a modified Marx generator setup in oil-immersed conditions. Five commercial cable types with differing insulation materials, jacket compositions, and voltage ratings were tested using a repeatable impulse testing protocol based on IEC 60229 and IEC 60060-1.

The theoretical framework included the design and adaptation of an impulse voltage generator, with specific attention to front and tail resistor configurations and capacitive divider calibration. Statistical evaluation of the breakdown data was performed using GEV analysis, thickness-normalized field strength calculations, and time-to-breakdown classification.

5.2 Overview of the Results

The statistical analysis conducted throughout this study played a central role in interpreting the dielectric performance of each cable type. Breakdown voltage data obtained from impulse testing were modeled using the GEV distribution, allowing for the extraction of percentile-based breakdown levels (U_{10}, U_{50}, U_{90}) that quantify both typical and worst-case behavior. This approach provided a probabilistic understanding of material performance rather than relying solely on maximum or average values, thereby offering a more realistic assessment of field-relevant reliability.

Among the tested cables, those with HDPE and PPS+HDPE jackets consistently exhibited higher U_{50} values and narrower percentile spreads, indicating more uniform and robust impulse withstand behavior. In contrast, PVC-jacketed cables, particularly Type A and Type E, showed lower breakdown voltages and broader Weibull distributions, pointing to greater variability and

reduced dielectric confidence under impulse stress. It should be noted, however, that Cable Type E is rated for 1 kV, which justifies to some extent its lower dielectric performance compared to the 20 kV-class cables evaluated in this study. Nevertheless, its high variability and sensitivity to impulse stress raise concerns regarding its oversheath design even within its voltage class.

A key finding of this study is that the absolute overvoltage levels at which breakdown occurred were generally modest and relatively consistent across all tested cables, often falling well below the withstand capabilities of the main insulation. This observation suggests that even moderate impulse stress may compromise the jacket, especially if the material is poorly suited or the thickness is insufficient. Despite this, existing standards and qualification frameworks have historically overlooked the jacket's impulse withstand capacity, focusing almost exclusively on mechanical and environmental protection. As the results here demonstrate, this omission represents a significant vulnerability: if the outer sheath is not properly dimensioned or selected, the cable may be exposed to dielectric failure long before the core insulation is ever challenged.

Beyond voltage levels, the analysis also incorporated a thickness-normalized breakdown field strength metric (kV/mm), which adjusted breakdown voltage data relative to each cable's jacket geometry. This enabled direct material comparisons regardless of construction differences. The results revealed that a thick jacket alone does not guarantee superior dielectric strength, performance depended heavily on compound formulation and material uniformity.

Additionally, breakdown timing was statistically categorized based on its location within the impulse waveform. Failures occurring during the front or tail portion of the waveform provided insight into each material's response to different transient characteristics. For example, PPS+HDPE jackets tended to fail later in the impulse, suggesting increased resilience to fast-rising electric field transients, whereas PVC jackets often failed during the early front, indicating a susceptibility to high dV/dt conditions.

Overall, the statistical analysis carried out in this thesis not only allowed for reliable comparisons between cable types but also exposed a critical gap in current design practices: the impulse withstand strength of the cable jacket is both quantifiable and essential. Ignoring this factor in standardization leaves medium-voltage systems vulnerable to failures that could be prevented through proper jacket selection and dimensioning.

5.3 Future Work

Building on the outcomes of this study, future research can expand in several key directions:

- **Expanded Material Library:** A wider range of commercial and developmental jacket compounds (e.g., LSZH, PUR, fluoropolymers) could be evaluated under identical conditions to further distinguish material-specific impulse responses.
- **Same Material, Different Geometry:** Applying the same jacket compound across different cable geometries and constructions would help isolate the effect of physical design on dielectric performance, offering a more comprehensive understanding of structure-property relationships.
- **Thermal and Mechanical Stress Coupling:** Future tests could introduce simultaneous thermal loading or mechanical flexing to simulate real-world stress scenarios encountered in buried or industrial installations.
- **Partial Discharge Onset Monitoring:** Integrating high-sensitivity partial discharge detection into the test circuit may enable early-stage degradation tracking prior to full dielectric failure, offering more detailed insights into jacket aging mechanisms.

In conclusion, this thesis provides a practical and statistically supported framework for evaluating MV cable jacket strength under high-voltage impulses and underscores the importance of tailoring outer sheath materials to transient-stress resilience, not just long-term thermal and mechanical performance.

CHAPTER 6: REFERENCES

[1] Electric Power Research Institute, EPRI Underground Transmission Systems Reference Book, Palo Alto, California: EPRI, 2006.

[2] T. Tanaka and A. Greenwood , Power Cable Technology, Volume II, Present and Future, Boca Raton, Florida: CRC Press, INC, 1983.

[3] International Electrotechnical Commission, "IEC 60502-2: Power cables with extruded insulation and their accessories for rated voltages from 1 kV (Um = 1,2 kV) up to 30 kV (Um = 36 kV) – Part 2: Cables for rated voltages from 6 kV (Um = 7,2 kV) up to 30 kV (Um = 36 kV)," IEC, Geneva, Switzerland, 2014.

[4] International Electrotechnical Commission, "IEC 60840: Power cables with extruded insulation and their accessories for rated voltages above 30 kV (Um = 36 kV) up to 150 kV (Um = 170 kV) – Test methods and requirments," IEC, Geneva, Switzerland, 2011.

[5] W. A. Thue, Electrical Power Cable Engineering, 3rd Edition, Boca Raton, Florida: CRC Press, 2017.

[6] CIGRE, "CIGRE TB 797 - Sheath bonding systems of AC transmission cables - Design, testing, and maintenance," CIGRE, Paris, France, 2020.

[7] BICC Cables Ltd, Electric Cables Handbook, London, U.K: Blackwell Science, 1997.

[8] International Electrotechnical Commision, IEC 60505: Evaluation and qualification of electrical insulation systems, Geneva, Switzerland: IEC, 2011.

[9] American Society for Testing and Materials, "D149 − 09 : Standard Test Method for Dielectric Breakdown Voltage and Dielectric Strength of Solid Electrical Insulating Materials at Commercial Power Frequencies," ASTM International, West Conshohocken, Pennsylvania, 2006.

[10] International Electrotechnical Commission, "IEC 60243-1: Electric strength of insulating materials – Test methods – Part 1: Tests at power frequencies," IEC, Geneva, Switzerland, 2013.

[11] International Electrotechnical Commission, "IEC 60270: High-voltage test techniques - Partial discharge measurements," IEC, Geneva, Switzerland, 2015.

[12] International Electrotechnical Commission, "IEC 60230: Impulse tests on cables and their accessories," IEC, Geneva, Switzerland, 2018.

[13] International Electrotechnical Commission, "IEC 60060-1 : High-voltage test techniques – Part 1: General definitions and test requirements," IEC, Geneva, Switzerland, 2010.

[14] Institute of Electrical and Electronics Engineers, "IEEE Std 400: IEEE Guide for Field Testing and Evaluation of the Insulation of Shielded Power Cable Systems Rated 5 kV and Above," IEEE, New York, USA, 2012.

[15] W. Z. J. K. E. Kuffel, High Voltage Engineering Fundamentals, Oxford, United Kingdom: Butterworth-Heinemann, 2000.

[16] American Society for Testing and Materials, "ASTM D1868−20: Standard Test Method for Detection and Measurement of Partial Discharge (Corona) Pulses in Evaluation of Insulation Systems," ASTM, West Conshohocken, Pennsylvania, U.S, 2020.

[17] International Electrotechnical Commission, "IEC 60230: Impulse tests on cables and their accessories," IEC, Geneva, Switzerland, 2018.

[18] International Electrotechnical Commission, "IEC 60229: Electric cables – Tests on extruded oversheaths with a special protective function," IEC , Geneva, Switzerland, 2007.

[19] International Electrotechnical Commission, "IEC 62230: Electric cables – Spark-test method," IEC, Geneva, Switzerland, 2006.

[20] Deutsche Industrie Norm, "VDE 0276-620: Power distribution cables with extruded insulation for rated voltages from 3.6/6 (7.2) kV up to and including 20.8/36 (42) kV," DIN, Berlin, Germany, 2024.

[21] International Electrotechnical Commission, "IEC 60296: Fluids for electrotechnical applications – Mineral insulating oils for electrical equipment," IEC, Geneva, Switzerland, 2020.

[22] EKO ABEE, "EKO INSULATING OIL - Transformer oil with antioxidant additives (inhibited)," EKO ABEE, Athens, Greece, 2019.

[23] S. Yuferev, L. Proekt and N. Ida, "Surface Impedance Boundary Conditions Near Corners and Edges: Rigorous Consideration," *IEEE TRANSACTIONS ON MAGNETICS,* p. 3465–3468, 5 September 2001.

[24] W. J. Carrey and J. R. Mayes, "Marx generator design and performance," in *Conference Record of the Twenty-Fifth International Power Modulator Symposium, 2002 and 2002 High-Voltage Workshop*, Austin, Texas, 2002.

[25] M. Naidu and V. Kamajaru, High Voltage Engineering, New Delhi, India: Tata McGraw-Hill, 1995.

[26] A. F. Andrade, E. G. Costa, A. B. Oliveira Neto, G. R. Lira and T. V. Ferreira, "Evaluation of statistical methods used in the estimation of breakdown voltage distribution.," IET Science, Measurement & Technology, Stevenage, United Kingdom, 2019.

[27] D. Fabiani and L. Simoni, "Discussion on Application of the Weibull Distribution to Electrical Breakdown of Insulating Materials," IEEE Transactions on Dielectrics and Electrical Insulation, Bologna, Italy, 2005.

[28] L. Zhao, G.-z. Liu, J.-c. Su, Y.-f. Pan and X.-b. Zhang, "Investigation of Thickness Effect on Electric Breakdown Strength of Polymers Under Nanosecond Pulses," *IEEE Transactions on Plasma Science,* pp. 3398 - 3508, 12 December 2011.

[29] V. M. Atrazhev, V. S. Vorob'ev, I. V. Timoshkin, M. J. Given and S. J. MacGregor, "Mechanisms of Impulse Breakdown in Liquid: The Role of Joule Heating and Formation of Gas Cavities," *IEEE Transactions on Plasma Science,* November 2010.

[30] International Electrotechnical Commission, "IEC 60183: Guidance for the selection of high-voltage A.C. cable systems," IEC, Geneva, Switzrland, 2015.